

NDVI-indicated long-term vegetation dynamics in Mongolia and their response to climate change at biome scale

Gang Bao,^{a,b} Yuhai Bao,^{a,*} Amarjargal Sanjjava,^c Zhihao Qin,^{b,d} Yi Zhou^b and Guang Xu^{e,f}

^a Inner Mongolia Key Laboratory of Remote Sensing and Geographic Information Systems, Inner Mongolia Normal University, Hohhot, China

^b International Institute for Earth System Science, Nanjing University, China

^c Institute of Geography, Mongolian Academy of Science, Ulaanbaatar, Mongolia

^d Institute of Agro-Resources and Regional Planning, Chinese Academy of Agricultural Sciences, Beijing, China

^e Institute of Geographic Sciences and Natural Resources Research, Chinese Academy of Sciences, Beijing, China

^f University of Chinese Academy of Sciences, Beijing, China

ABSTRACT: Based on the vegetation map of Mongolia, Global Inventory Monitoring and Modelling Studies (GIMMS) normalized difference vegetation index (NDVI) (1982–2006), the Moderate Resolution Imaging Spectroradiometer (MODIS) NDVI (2000–2010), and temperature and precipitation data derived from 60 meteorological stations, this study has thoroughly examined vegetation dynamics in Mongolia and their responses to regional climate change at biome scale. To ensure continuity and consistency between the two NDVI datasets, the MODIS NDVI was first calibrated to the GIMMS NDVI based on the overlapping period of 2000–2006. Good calibration results with R^2 values of 0.86–0.98 between the two NDVI datasets were obtained and can detect subtle trends in the long-term vegetation dynamics of Mongolia. The results indicated that for various biomes, although NDVI changes during 1982–2010 showed great variation, vegetation greening for all biomes in Mongolia seem to have stalled or even decreased since 1991–1994, particularly for meadow steppe (0.0015 year^{-1}), typical steppe ($-0.0010 \text{ year}^{-1}$), and desert steppe ($-0.0008 \text{ year}^{-1}$), which is an apparent turning point (TP) of the vegetation growth trend in Mongolia. A pronounced drying trend (from $-4.399 \text{ mm year}^{-1}$ in meadow steppe since 1990 to $-2.445 \text{ mm year}^{-1}$ in alpine steppe since 1993) occurred between 1990 and 1994, and persistently warming temperatures ($0.015 \text{ }^{\circ}\text{C year}^{-1}$ in alpine steppe to $0.070 \text{ }^{\circ}\text{C year}^{-1}$ in forest and meadow steppe) until recently have likely played a major role in this NDVI trend reversal. However, the NDVI TP varied by biome, month, and climate and was not coupled exactly with climatic variables. The impact on climate of both same-time and lagged-time temperature and precipitation effects also varied strongly across biomes and months. On the whole, climate-related vegetation decline and associated potential desertification trends will likely be among the major sources of ecological pressure for each biome in Mongolia, which could intensify environmental problems like sandstorms in other East Asian regions.

KEY WORDS climate change; vegetation dynamics; NDVI; Mongolia; biome scale

Received 10 August 2014; Revised 2 January 2015; Accepted 16 January 2015

1. Introduction

Vegetation not only serves as a direct indicator of the status of terrestrial ecosystems as well as local and global environmental changes (Potter *et al.*, 2008; Jiang *et al.*, 2013) but also regulates the carbon cycle, energy exchange, and climate change in the Earth's systems in direct and indirect ways, including photosynthesis, surface albedo, evapotranspiration, and roughness (Wang *et al.*, 2011; Chen *et al.*, 2014). Regional vegetation history is generally regarded as a footprint of climate variations and provides an excellent opportunity to examine climate change impacts on ecosystems through time, space, or both (Huntley and Webb, 1988; Whitlock and Bartlein, 1997). Therefore, vegetation dynamics and their response to global climate change (focusing mostly on precipitation

and temperature) have increasingly become a main focus of global change studies, particularly since the 1980s when the satellite-derived normalized difference vegetation index (NDVI) became available (Myneni *et al.*, 1997; Tucker *et al.*, 2001; Zhou *et al.*, 2001; Nemani *et al.*, 2003; Potter *et al.*, 2008; Piao *et al.*, 2011; Wang *et al.*, 2011; Chen *et al.*, 2014). Most of these studies have generally suggested that vegetation photosynthetic activity (NDVI) in northern high latitudes increased from the 1980s to the 1990s with increases in temperature (Myneni *et al.*, 1997; Tucker *et al.*, 2001; Zhou *et al.*, 2001; Nemani *et al.*, 2003; Piao *et al.*, 2006a). However, studies on continental or global scales may neglect small-scale heterogeneity to some extent if national or local heterogeneity has not had a decisive effect on continental or global vegetation dynamics because these studies miss a certain amount of local detail due to the coarse spatial resolution of Global Inventory Monitoring and Modelling Studies (GIMMS) NDVI data and differences in observation period (Walther *et al.*, 2002; Rocchini, 2007; Yao *et al.*, 2012). In addition,

* Correspondence to: Y. Bao, Inner Mongolia Key Laboratory of Remote Sensing and Geographic Information Systems, Inner Mongolia Normal University, Hohhot, China. E-mail: baoyuhai@imnu.edu.cn

vegetation dynamics and their responses to climate change have varied considerably due to different ecogeographical conditions (Chuai *et al.*, 2013), and therefore examining the effect of climate on vegetation dynamics at the biome scale, particularly at finer temporal scales (such as monthly or even shorter timescales), could gain further insight into the mechanisms of interaction between climate and vegetation variability (Chen *et al.*, 2014).

The Republic of Mongolia lies in a transitional zone from the Gobi Desert of central Asia in the southwest to the Siberian taiga forest in the north (Li *et al.*, 2008). Most of the Mongolian territory is characterized by arid and semiarid climate, and over 70% of Mongolia is covered by high-quality steppe grasslands (Fernandez-Gimenez and Allen-Diaz, 2001) with high sensitivity to global climate change (Watson and Albritton, 2001). As in other (semi)arid regions, although precipitation is the primary climatic control on vegetation activity at a national scale (Myneni *et al.*, 1997; Zhou *et al.*, 2001; Zemmrich *et al.*, 2010) and may even overcome the negative effects of grazing intensity (Zemmrich *et al.*, 2010), the relatively complex contribution of vegetation-related climatic variables to vegetation dynamics may be regionally dependent and may vary strongly by biome. Therefore, it is hypothesized here that vegetation dynamics, particularly at biome scales, and their response to climate change in Mongolia may not be completely consistent with the results of studies conducted in areas where temperature is a more important factor in plant growth. Furthermore, compared to other regions in northern high latitudes, the intensity of climate warming in Mongolia has tended to be greater than the global average (Serreze *et al.*, 2000; Lu *et al.*, 2009). This would severely aggravate drought stress without a concurrent increase in rainfall, restricting plant growth and even intensifying desertification tendencies and other related disasters like sandstorms and soil erosion (Zou and Zhai, 2004). In addition, the population of Mongolia was 2.83 million in 2011, with the lowest density in the world, 1.8 persons per square kilometre (National Statistical Office of Mongolia, 2011), and nomadic herding has been the predominant Mongolian economic activity from ancient times until now (Neupert, 1999). This situation leads to minimal human impact on the ecosystem and recommends Mongolia as an ideal region for exploring the mechanisms of interaction between climate change and vegetation dynamics. However, very few studies (Zhang *et al.*, 2009; Eckert *et al.*, 2015) on nation-scale vegetation dynamics in Mongolia have been performed over the past three decades, despite the ecological and geographical significance of Mongolia, such as its role as a birthplace of sandstorms (Fujiwara *et al.*, 2007).

One of the common ways to explore vegetation changes and their response to climate change is to use the satellite-derived NDVI (Myneni *et al.*, 1997; Nemani *et al.*, 2003; Chen *et al.*, 2014) because NDVI is highly correlated with photosynthetically active biomass, leaf area, chlorophyll abundance, and potential photosynthesis of vegetation (Nemani *et al.*, 2003; Schmidt *et al.*, 2014). It is based on the contrast between the

absorption in the red band due to vegetation chlorophyll pigments and the reflection in the infrared band caused by leaf cellular structure and is calculated as $NDVI = (NIR - RED) / (NIR + RED)$, where RED and NIR represent the reflectance in the red and near-infrared band, respectively (Ruse *et al.*, 1974). Although NDVI has several limitations, including saturation in a densely vegetated canopy and an intensively noisy canopy background signal in sparsely vegetated regions (Huete *et al.*, 2002), it is widely used in vegetation dynamics studies from local to global scales after processing to monthly maximum composite values, which can greatly reduce noise (Nemani *et al.*, 2003; Zhang *et al.*, 2013), particularly in northern latitudes (Myneni *et al.*, 1997; Tucker *et al.*, 2001). At present, although a number of NDVI datasets such as GIMMS NDVI (three generations), MODIS NDVI, and SPOT VGT NDVI have become available, no single NDVI time series covers the past three decades at large spatial extent except for GIMMS NDVI3g (Eastman *et al.*, 2013; Chen *et al.*, 2014). Therefore, there is a great need to combine the new NDVI time-series dataset from MODIS with the traditional GIMMS NDVI by developing a cross-calibration method between different NDVI datasets from different sensors (Steven *et al.*, 2003; Mao *et al.*, 2012). This would make it possible to extend vegetation dynamics measurements through time, particularly for future measurements, although GIMMS NDVI3g has become available recently (Eastman *et al.*, 2013; Chen *et al.*, 2014).

The objectives of the present study are (1) to develop an NDVI time series for the Mongolian ecosystem covering 1982–2010 by calibrating the MODIS NDVI (2000–2010) to the GIMMS NDVI (1982–2006) based on the overlapping period of 2000–2006; (2) to investigate what vegetation dynamics have occurred over the past 29 years at biome scales, and for what reasons, using a least-squares linear regression model (Zhou *et al.*, 2001) and a piecewise regression approach (Chen *et al.*, 2014); and (3) to examine NDVI variations and the turning point (TP) of NDVI trends for each month to detect the contribution of monthly NDVI to growing-season NDVI, and also to examine the monthly lagged impacts of climatic variables on vegetation dynamics at a biome scale, based on the vegetation map of Mongolia.

2. Data and methods

2.1. Study area

Mongolia is located in the heart of central Asia and stretches from approximately 41°–52°N and 81°–119°E, with an area of approximately 156×10^4 km² (Figure 1). The climatic regime is characterized by a typical continental climate, with annual precipitation ranging between 50 mm in the southwestern Gobi Desert area and 350 mm in the northern forested region. The temperature gradient slopes in the opposite sense to that of precipitation, ranging from less than 1.5 °C in the northern mountains to over 16 °C in the southwestern Gobi Desert. Mongolia has

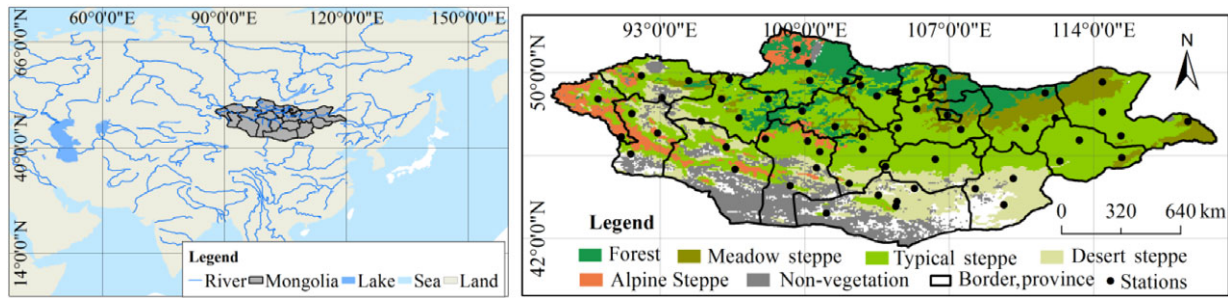


Figure 1. Location of study area and distribution of biomes and meteorological stations.

one of the largest undeveloped grassland ecosystems in the world (Lu *et al.*, 2009) except for the northern forested area and the southwestern Gobi Desert, and all these ecosystems are very sensitive to climate change (Li *et al.*, 2008). Under the influence of climatic differentiation, vegetation across Mongolia displays an obvious latitudinal zonation, passing through forest, meadow steppe, typical steppe, desert steppe, and the Gobi Desert from north to south and from northeast to southwest. Alpine steppe is also distributed in the northern and western mountain ranges (Figure 1).

2.2. Dataset

NDVI datasets produced by the GIMMS group using the Advanced Very High Resolution Radiometer (AVHRR)/the National Oceanic and Atmospheric Administration (NOAA) series satellites (NOAA 7, 9, 11, 14, 16, 17, and 18) and the MOD12C1 NDVI product (Level-3 product) derived from the Terra MODIS instrument were used in the present study. The GIMMS NDVI covers the period from 1982 to 2006 and has a resolution of 8 km and an interval of 15 days, whereas the MODIS NDVI covers the period from 2000 to 2010 and has a resolution of 5.6 km and an interval of 16 days. These two NDVI datasets have been corrected to remove noise from solar angle and sensor errors and have been widely used in studies on monitoring of long-term vegetation activity from regional to global scales (Nemani *et al.*, 2003; Mao *et al.*, 2012). To decrease some non-vegetation effects further, a monthly NDVI dataset was generated for both GIMMS and MODIS NDVI by applying the maximum value composite (MVC) method (Holben, 1986) to the two NDVI images for each growing-season month. To match the spatial resolution of the GIMMS NDVI, the MODIS NDVI was then further spatially resampled to 8 km. The growing season was defined as from April to October, and growing-season NDVI data were obtained by averaging monthly NDVI data from April to October for each year (Piao *et al.*, 2011). The growing-season average NDVI can phenologically be regarded as the average measurable level of photosynthetic activity during 1 year (Chen *et al.*, 2014), which is a meaningful indicator of interannual vegetation dynamics at regional scale (Chuai *et al.*, 2013).

The climate variables used were the growing-season monthly precipitation amount and the mean temperature derived from 60 meteorological stations across Mongolia,

as provided by the Mongolian Weather Bureau and the Institute of Geography, Mongolian Academy of Science. According to the locations of the meteorological stations, monthly climatic data were interpolated in the ArcGIS environment using the kriging method at a spatial resolution of 8 km to match both temporally and spatially the time sequences of growing-season mean NDVI. Although some errors may have resulted from the areal interpolation due to the limited number of meteorological stations available (Piao *et al.*, 2003), previous studies have demonstrated that kriging is a better interpolation method with higher accuracy and lower bias than other methods (Li *et al.*, 2005; Wu and Li, 2013), particularly in areas with uniformly distributed climate stations (Figure 1) and having minimal elevation changes and subdued topography (mostly grassland ecosystems) like Mongolia.

Vegetation data were obtained from the vegetation map in the National Atlas of Mongolia (Institute of Geography, Mongolian Academy of Science, 2009). The vegetation map was first scanned, geometrically corrected, and digitized using the ArcGIS software and then rasterized at 8 km, as was done for the NDVI and climatic datasets. Vegetation types in Mongolia were further grouped into forest, meadow steppe, typical steppe, desert steppe, and alpine steppe. Cropland and Gobi Desert vegetation were neglected in the present study because the first accounted for a very small number of pixels in the 8-km GIMMS NDVI data and the second consisted of very sparse vegetation. As was done in a study at the whole China scale (Piao *et al.*, 2003), it is hypothesized here that the five broad vegetation types (without considering subtypes) mentioned earlier are relatively stable and that this study can ignore land conversion between broad vegetation types in 8-km coarse spatial resolution NDVI images over the study period, primarily due to the long prevalence of nomadic herding in Mongolia, the low population density, and the associated minimal human disturbance (Neupert, 1999; Upton, 2010).

2.3. Method

2.3.1. Calibrating MODIS NDVI to GIMMS NDVI

To study long-term vegetation response to climate change, there is a strong need to combine NDVI data from more than one sensor to cover a sufficiently long time period (Steven *et al.*, 2003; Mao *et al.*, 2012). However, due to

differences among satellites, sensor designs, and resolutions, it is necessary to calibrate from one NDVI product to another and to check the consistency between them (Brown *et al.*, 2008). In the present study, numerous linear regression models (for each pixel) (Equation (1)) were developed to calibrate MODIS NDVI to GIMMS NDVI for each month of the growing season during 2000–2010 by regressing GIMMS NDVI as a function of MODIS NDVI for the overlapping period of 2000–2006:

$$G(k, m) = a(k, m)M(k, m) + b(k, m) + \varepsilon(k, m) \quad (1)$$

where $G(k, m)$ and $M(k, m)$ are the GIMMS NDVI and the MODIS NDVI of pixel k in month m , a and b are the regression coefficients (slope and intercept) obtained by fitting time series to the two NDVIs for each month of 2000–2006, and ε is the residual error. By applying the developed models, a new monthly MODIS NDVI dataset from 2000 to 2010 (called the Extended GIMMS NDVI in the following discussion), which has similar characteristics to the GIMMS NDVI, was generated to extend the traditional GIMMS NDVI up to the present. The correlation analysis and difference values between the 2 monthly NDVI for each biome were examined to evaluate whether consistency had been attained.

2.3.2. Vegetation dynamics and its response to climate change

Based on the vegetation map, time series for growing-season mean NDVI [both GIMMS NDVI (1982–2006) and extended GIMMS NDVI (2000–2010)], temperature, and precipitation and also for monthly NDVI, temperature, and precipitation during 1982–2010 were constructed for each biome by averaging all grid pixels belonging to the same biome. Subsequently, a least-squares linear regression model and a piecewise linear regression model were used to detect vegetation and climate variations during 1982–2010.

The least-squares linear regression model (Piao *et al.*, 2011; Chen *et al.*, 2014) was used to detect gradual trends in the NDVI time series and in climatic variables during the 29-year period (Equation (2)):

$$y = a + bt + \varepsilon \quad (2)$$

where y represents the NDVI time series, t is the year, a is the intercept, b is the linear trend (slope), and ε is the residual of the fit.

Generally, trends in long-term NDVI and climatic data might change or reverse in a particular year (Zhang *et al.*, 2013; Chen *et al.*, 2014). A piecewise linear regression model (Toms and Lesperance, 2003; Tomé and Miranda, 2004) was used to detect the timing and magnitude of potential trend changes in NDVI and climatic variables (Equation (3)):

$$y = \begin{cases} a_0 + b_1t + \varepsilon & t \leq \alpha \\ a_0 + b_1t + b_2(t - \alpha) + \varepsilon & t > \alpha \end{cases} \quad (3)$$

where y is the NDVI or climatic variable time series, t is the year, α is the estimated TP of the time-series trend;

a_0 , b_1 , and b_2 are the regression coefficients; a_0 is the intercept, b_1 and $b_1 + b_2$ are the trends before and after the TP, and ε is the residual error. In the present study, the condition $\alpha \in \{4, 6, \dots, N - 4\}$ was imposed to eliminate two consecutive segments before and after the TP with too few data points, as done in a previous study (Chen *et al.*, 2014). The TP was estimated by the maximum likelihood method.

The two models described above were implemented for the NDVI and climatic variables over the growing-season and monthly timescales for each biome. To examine the climatic factors driving the changes in NDVI trends, the Pearson correlation coefficients and p -values (significance level) between NDVI and climatic variables were calculated for each biome. In view of the lagged response of NDVI to climatic variables, the correlations between monthly NDVI and temperature and precipitation for all previous growing-season months in a calendar year were also calculated.

3. Results and discussion

3.1. Calibration from MODIS NDVI to GIMMS NDVI

The scatter plots between growing-season monthly GIMMS NDVI and Extended GIMMS NDVI by biome are shown in Figure 2(a) [7 months (April–October) \times 7 years (2000–2006) = 49 points for each biome]. The results showed high coefficients of determination between the GIMMS NDVI and the new Extended GIMMS NDVI for all biomes, with values around 0.98 except for desert steppe (0.86), a result comparable to those from previous studies (Brown *et al.*, 2008; Mao *et al.*, 2012). The relatively lower R -value for desert steppe was mostly attributable to lower intra-annual NDVI variation in this environment (Fensholt and Proud, 2012). The standard deviation of multi-year average monthly NDVI was lowest for desert steppe (0.009) (Table 1). Another reason for this lower R -value may be the difference between reflectance in the red and near-infrared bands in sparsely vegetated regions like desert steppe when calculating the MODIS NDVI and the GIMMS NDVI (Steven *et al.*, 2003; Fensholt *et al.*, 2009). It is well known that the soil background has a large impact on the reflected signal from a sparsely vegetated region (Fensholt *et al.*, 2009), and the large reflectance difference between the red and near-infrared bands therefore stands out at lower canopy cover (Huete, 1988). The difference values between the two NDVI datasets were mostly concentrated between -0.03 and 0.03 (Figure 2(b)), indicating high consistency and continuity between the two datasets. The high degree of continuity and consistency between the two NDVI datasets can also be clearly observed in Figure 3.

3.2. Interannual variations in growing-season mean NDVI and climatic variables

Figure 3 and Table 2 show the interannual variation of growing-season mean NDVI, temperature, and total

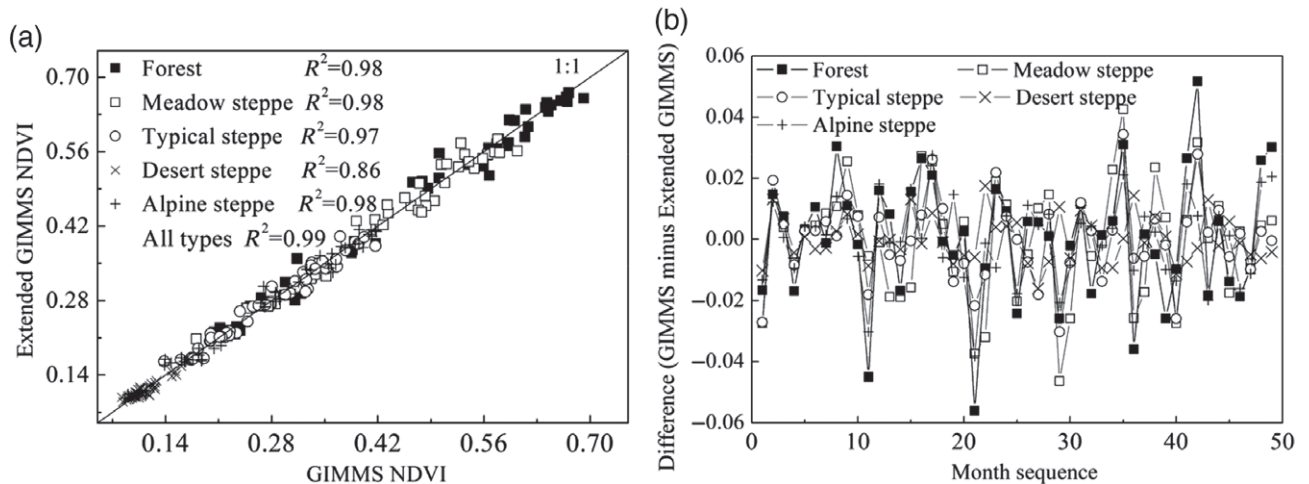


Figure 2. Calibration result from MODIS NDVI to GIMMS NDVI.

Table 1. Standard deviation of multi-year average monthly NDVI by biome.

	Forest	Meadow steppe	Typical steppe	Desert steppe	Alpine steppe
SD	0.161	0.127	0.072	0.009	0.106

precipitation during 1982–2010 in Mongolia for forest, meadow steppe, typical steppe, desert steppe, and alpine steppe. For the entire observation period, the vegetation activity of forest and alpine steppe experienced a significant increasing trend, with annual increments in mean NDVI values of 0.0007 year^{-1} ($p=0.03$) and 0.0009 year^{-1} ($p=0.0003$) (Figure 3(a) and (e)). However, the curves for meadow steppe, typical steppe, and desert steppe vegetation remained nearly flat, and no obvious trend was observed (trend = 0.0001, 0.0001, and $-0.00002 \text{ year}^{-1}$ for meadow steppe, typical steppe, and desert steppe, respectively) over a 29-year period (Figure 3(b)–(d); Table 2). All the piecewise linear models based on 29-year time-series NDVI data predicted a TP year for NDVI trend of 1994 (Figure 3(b)–(e); Table 2), except for forest, where the TP was predicted to occur in 1991 (Figure 3(a)). For the four steppe grassland ecosystems, the NDVI gradually increased until 1994, with the largest increase (0.0025 year^{-1}) occurring in meadow steppe and the lowest (0.0011 year^{-1}) in desert steppe; all these trends then stalled or decreased at a rate of $-0.00002 \text{ year}^{-1}$ (alpine steppe) to $-0.0015 \text{ year}^{-1}$ (meadow steppe). Forest vegetation increased until 1991 at a rate of 0.0025 year^{-1} and showed a flat trend afterward ($0.00006 \text{ year}^{-1}$). This NDVI trend reversal, particularly for meadow steppe, typical steppe, and desert steppe in Mongolia over a 29-year period, is generally consistent with the results of previous studies conducted in the rest of Eurasia and in North America based on shorter data series (1982–2006, 25 years) (Park and Sohn, 2010; Piao *et al.*, 2011; Wang *et al.*, 2011), which demonstrated that the increasing trends in vegetation growth before the late

1990s seem to have stalled or even reversed from that time onward. However, the reversal in Mongolia seems to have occurred about 3–6 years earlier than in the rest of Eurasia and in North America.

Climate records in Mongolia show warming and drying trends for all biomes from 1982 to 2010 (Figure 3), indicating that drought stress and potential desertification stress are major environmental issues in Mongolia. Particularly for forest, meadow steppe, and typical steppe, the increasing temperature trend and the decreasing precipitation trend were both significant at the 1% level (Figure 3(a)–(c)). The piecewise regression model further indicated that pronounced drying trends for most biomes occurred between 1990 and 1994, followed by persistent warming trends until recently. Detailed information including trends, TPs, and intercepts of all modelled vegetation and climate variations can also be clearly seen in Table 2.

3.3. Response of growing-season NDVI to climate change

It can be clearly seen from Table 3 that the relationship between growing-season mean NDVI and climatic variables from the corresponding period strongly varied among biomes, depending mostly on differences in the climate limiting factor for plant growth in the different biomes. For forest, regardless of the observation period, growing-season NDVI was positively correlated with temperature, particularly for the entire observation period ($R=0.47$, $p=0.009$), but negatively with precipitation ($R=-0.34$, $p=0.07$), indicating that against the background of global warming, rising temperatures were beneficial to forest growth in Mongolia during the previous 29-year period. This observation is in agreement with previous studies suggesting that temperature is a decisive climatic factor for vegetation growth in northern high latitudes (Zhou *et al.*, 2001; Ichii *et al.*, 2002; Nemani *et al.*, 2003) and that an increase in temperature could enhance forest growth by lengthening the growing period and enhancing photosynthesis (Zhou *et al.*, 2001; Piao

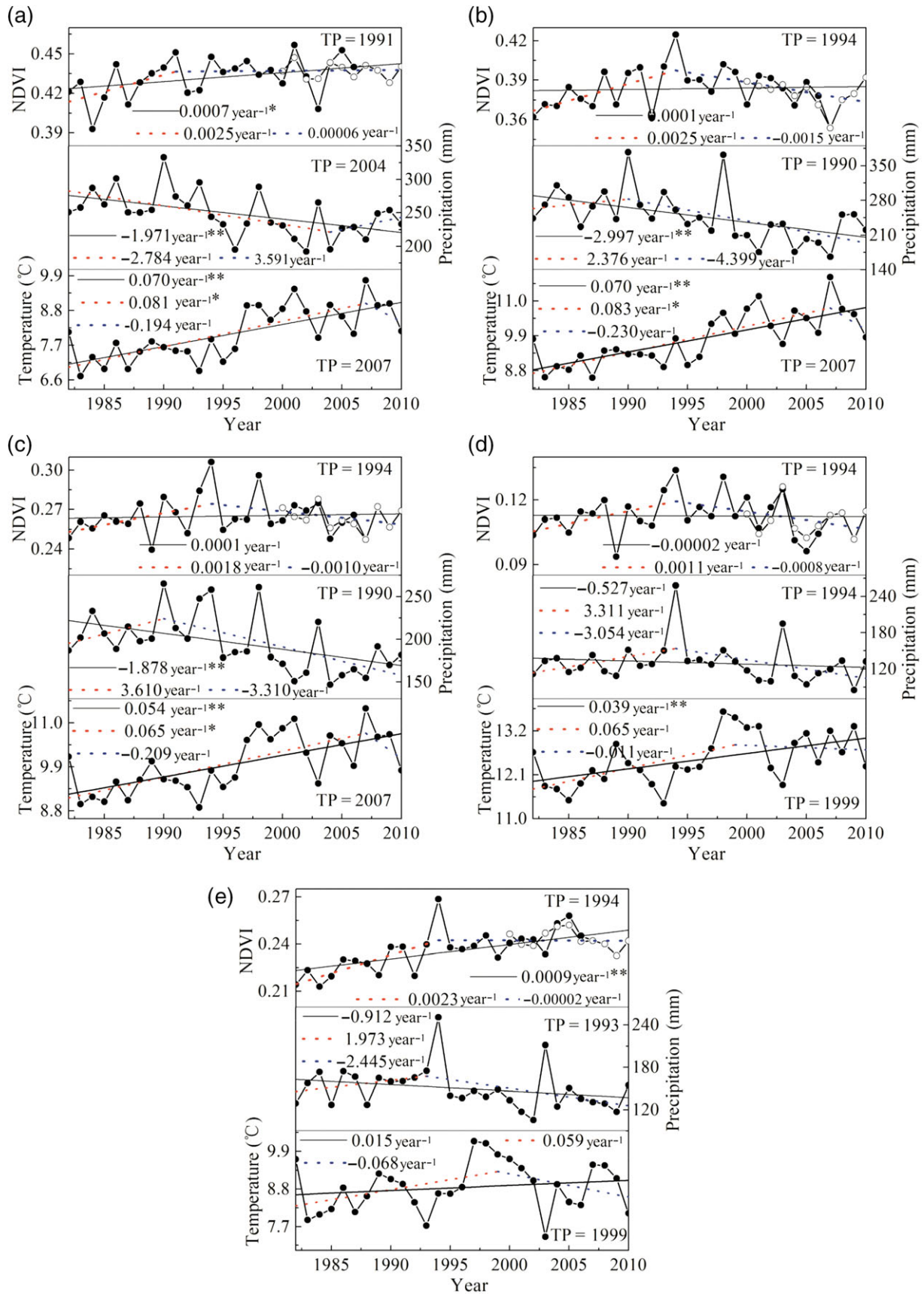


Figure 3. Interannual variations of growing-season mean NDVI, temperature, and precipitation from 1982–2010 for (a) forest, (b) meadow steppe, (c) typical steppe, (d) desert steppe, and (e) alpine steppe. The extended GIMMS NDVI is indicated by the symbol \circ . ** and * indicate $p < 0.01$, $p < 0.05$ respectively.

Table 2. Linear regression models and piecewise linear regression models for 1982–2010 by biome. y_n , y_p , and y_t represent NDVI, precipitation, and temperature, respectively, and t represents the year.

Biome	Linear regression models	Piecewise linear regression models
Forest	$y_n = -0.9309 + 0.0007t$ $y_p = 4183.02 - 1.971t$ $y_t = -131.71 + 0.070t$	$y_n = \begin{cases} -4.578 + 0.0025t & t \leq 1991 \\ -4.578 + 0.0025t - 0.0025(t - 1991) & t > 1991 \end{cases}$ $y_p = \begin{cases} 5802.18 - 2.785t & t \leq 2004 \\ 5802.18 - 2.785t + 6.376(t - 2004) & t > 2004 \end{cases}$ $y_t = \begin{cases} -153.29 + 0.081t & t \leq 2007 \\ -153.29 + 0.081t - 0.275(t - 2007) & t > 2007 \end{cases}$
Meadow steppe	$y_n = 0.163 + 0.0001t$ $y_p = 6231.46 - 2.998t$ $y_t = -130.76 + 0.070t$	$y_n = \begin{cases} -4.683 + 0.0025t & t \leq 1994 \\ -4.683 + 0.0025t - 0.0040(t - 1994) & t > 1994 \end{cases}$ $y_p = \begin{cases} -4446.3 + 2.376t & t \leq 1990 \\ -4446.3 + 2.376t - 6.776(t - 1990) & t > 1990 \end{cases}$ $y_t = \begin{cases} -155.28 + 0.083t & t \leq 2007 \\ -155.28 + 0.083t - 0.313(t - 2007) & t > 2007 \end{cases}$
Typical steppe	$y_n = 0.028 + 0.0001t$ $y_p = 3944.95 - 1.878t$ $y_t = -97.808 + 0.054t$	$y_n = \begin{cases} -3.255 + 0.0018t & t \leq 1994 \\ -3.255 + 0.0018t - 0.0027(t - 1994) & t > 1994 \end{cases}$ $y_p = \begin{cases} -6959.39 + 3.609t & t \leq 1990 \\ -6959.39 + 3.609t - 6.919(t - 1990) & t > 1990 \end{cases}$ $y_t = \begin{cases} -119.26 + 0.065t & t \leq 2007 \\ -119.26 + 0.065t - 0.273(t - 2007) & t > 2007 \end{cases}$
Desert steppe	$y_n = 0.157 - 0.00002t$ $y_p = 1181.95 - 0.527t$ $y_t = -64.569 + 0.039t$	$y_t = \begin{cases} -2.171 + 0.0011t & t \leq 1994 \\ -2.171 + 0.0011t - 0.0019(t - 1994) & t > 1994 \end{cases}$ $y_p = \begin{cases} -6449.14 + 3.311t & t \leq 1994 \\ -6449.14 + 3.311t - 6.356(t - 1994) & t > 1994 \end{cases}$ $y_t = \begin{cases} -117.40 + 0.065t & t \leq 1999 \\ -117.40 + 0.065t - 0.077(t - 1999) & t > 1999 \end{cases}$
Alpine steppe	$y_n = -1.575 + 0.0009t$ $y_p = 1971.6 - 0.913t$ $y_t = -21.107 + 0.015t$	$y_n = \begin{cases} -4.383 + 0.0023t & t \leq 1994 \\ -4.383 + 0.0023t - 0.0023(t - 1994) & t > 1994 \end{cases}$ $y_p = \begin{cases} -3764.4 + 1.973t & t \leq 1993 \\ -3764.4 + 1.973t - 4.417(t - 1993) & t > 1993 \end{cases}$ $y_t = \begin{cases} -108.42 + 0.059t & t \leq 1999 \\ -108.42 + 0.059t - 0.127(t - 1999) & t > 1999 \end{cases}$

Table 3. Correlations between growing-season NDVI and climate variables for different biomes: growing-season precipitation (P), growing-season temperature (T); ESP, BTP, ATP represent the entire study period, before the turning point, and after the turning point.

Biome	Precipitation			Temperature		
	ESP	BTP	ATP	ESP	BTP	ATP
Forest	-0.34*	0.26	-0.41*	0.47***	0.36	0.32
Meadow steppe	0.35*	0.35	0.52**	-0.11	0.30	-0.51**
Typical steppe	0.62***	0.73***	0.85***	-0.08	-0.14	-0.19
Desert steppe	0.74***	0.78***	0.79***	-0.17	-0.32	-0.20
Alpine steppe	0.15	0.77***	0.43*	0.13	-0.02	-0.15

***, **, and * indicate $p < 0.01$, $p < 0.05$, and $p < 0.1$, respectively.

et al., 2011). However, excessive precipitation may restrict forest growth due to precipitation-accompanied reductions in solar radiation and temperature (Mao *et al.*, 2012).

In contrast, there were significant positive correlations between NDVI and precipitation for meadow steppe ($R = 0.35$, $p = 0.06$), typical steppe ($R = 0.62$, $p = 0.0004$), and desert steppe ($R = 0.74$, $p < 0.0000$), but negative correlations between NDVI and temperature ($R = -0.11$,

$p = 0.57$; $R = -0.08$, $p = 0.67$; $R = -0.17$, $p = 0.39$) for the same biomes from 1982 to 2010 (Table 3). Moreover, the patterns of NDVI fluctuation, particularly for typical steppe (Figure 3(c)) and desert steppe (Figure 3(d)), corresponded closely to that of precipitation. Peak NDVI values observed in 1990, 1994, 1998, and 2003 corresponded closely to peak precipitation in the same year, and lower NDVI values in 1982, 1992, 1995, 1999, 2004, and 2007

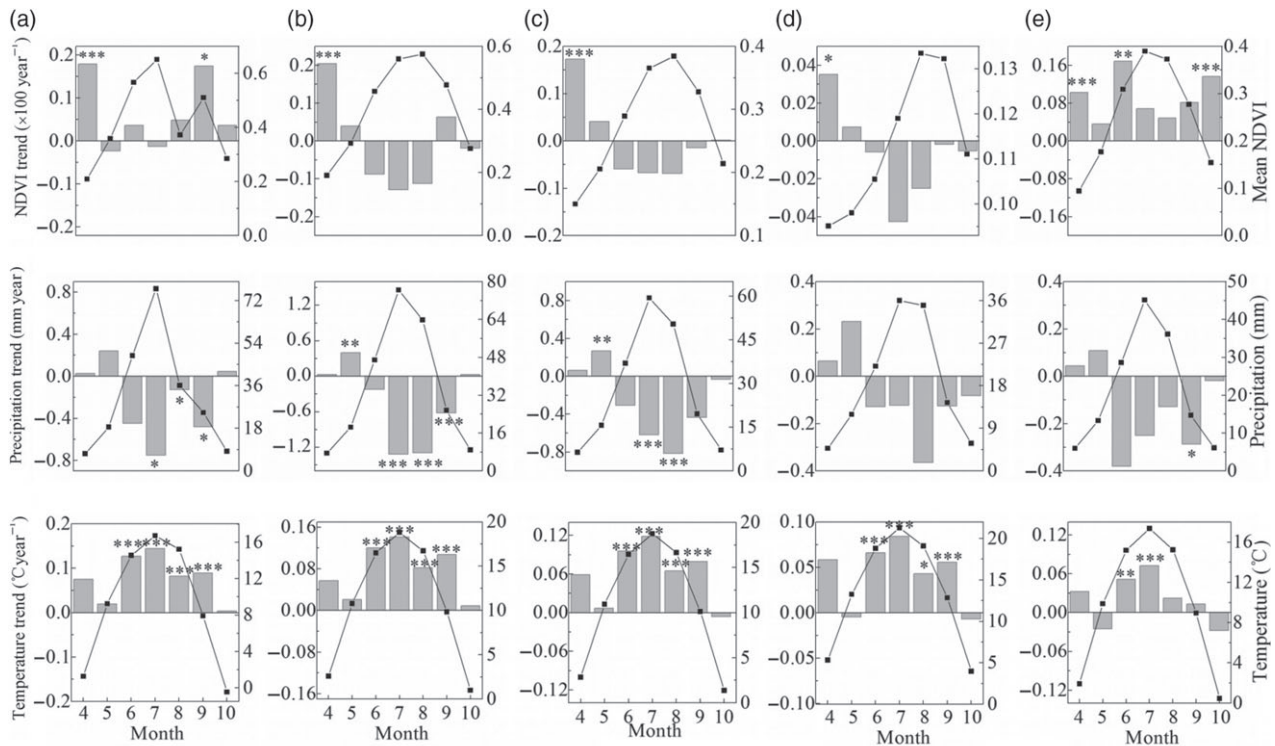


Figure 4. Dynamics of monthly NDVI and climatic variables from 1982 to 2010 for five biome types: (a) forest, (b) meadow steppe, (c) typical steppe, (d) desert steppe, and (e) alpine steppe. The bars represent trends, and the lines denote mean values. ***, **, and * indicate $p < 0.01$, $p < 0.05$, and $p < 0.1$, respectively.

corresponded well with lower precipitation, implying that rainfall is a direct factor regulating vegetation variation in grasslands, an observation which is in agreement with previous findings (Hoffmann and Jackson, 2000; Piao *et al.*, 2006b). In addition, positive correlations with precipitation increased obviously from meadow steppe to typical steppe and then to desert steppe, implying that the sensitivity of vegetation to precipitation may increase in extremely arid regions as aridity increases. However, against the background of global warming, the heat conditions are sufficient for grass growth in steppe-dominated regions in Mongolia, and rising temperatures could increase drought stress and thereby restrict grass growth (negative correlation). For alpine steppe, the effects of precipitation on vegetation dynamics seem to be stronger than those of temperature on both sides of the TP but are not obvious over the entire study period (Table 3).

Generally, the TPs of the growing-season mean NDVI trends were not always coupled with those of climatic variables (Figure 3, Table 2). For forest, the TPs of climatic variables, both temperature and precipitation, arrived later than that of NDVI. However, for steppe grassland ecosystems, the TP of precipitation occurred earlier than that of NDVI, whereas the TP of temperature arrived later than that of NDVI. These findings suggested that perhaps the TP of NDVI as detected by the piecewise linear regression model may be very complex and attributable to the combined influence of numerous variables, not only temperature and precipitation but also other climatic and non-climatic factors.

3.4. Response of monthly NDVI to climate change

3.4.1. Dynamics of monthly NDVI and climatic variables

Variations in growing-season NDVI can be attributed mostly to trends in monthly NDVI (Piao *et al.*, 2003), and monthly scale analysis can detect more detailed NDVI change signals and their contribution to growing-season NDVI trend (Chen *et al.*, 2014). Figure 4 shows the mean values and change trends of monthly NDVI over 1982–2010 by biome in Mongolia. For forest, the NDVI trends for all months increased except for May and July, with the largest increases occurring in April (trend: 0.0018 year^{-1} , $R = 0.60$, $p = 0.0007$) and September (trend: 0.0017 year^{-1} , $R = 0.34$, $p = 0.07$) (Figure 4(a), top), implying that the forest ecosystem in Mongolia tends to exhibit an earlier start of the growing season and delayed dormancy (i.e. lengthening of the growing season) (Zhou *et al.*, 2001; Park and Sohn, 2010; Piao *et al.*, 2011). This observation is also in agreement with others made in forest in China by Piao *et al.* (2003), who found that the largest increases in forest NDVI in China took place mostly in April, May, and September. By comparison, NDVI values for meadow steppe, typical steppe, and desert steppe significantly increased in April by 0.0021 year^{-1} ($R = 0.75$, $p < 0.0000$), 0.0017 year^{-1} ($R = 0.78$, $p < 0.0000$), and 0.0004 year^{-1} ($R = 0.36$, $p = 0.05$), respectively, and decreased in almost all summer and autumn months (Figure 4(b)–(d), top). However, the NDVI values for all growing-season months increased

Table 4. TPs of monthly NDVI, temperature, and precipitation during 1982–2010.

	April	May	June	July	August	September	October
Forest							
NDVI	1985	1990	1985	1985	1988	1985	1995
Precipitation	1985	2003	2005	1993	2006	1991	1996
Temperature	2007	2006	2002	2002	2007	1992	1985
Meadow steppe							
NDVI	1989	2001	1985	1988	1990	1996	1998
Precipitation	2004	2007	2005	1990	2006	1990	1987
Temperature	2007	2006	1989	2002	2007	1992	2000
Typical steppe							
NDVI	1989	2002	1988	1990	1994	1996	1998
Precipitation	1985	1988	2005	1993	1990	1991	2005
Temperature	2007	2000	2001	2000	2007	1992	1985
Desert steppe							
NDVI	1989	2001	2000	1994	1994	1994	1998
Precipitation	2007	2003	1994	1994	1994	2007	2005
Temperature	2007	2000	2001	2000	2001	1985	1986
Alpine steppe							
NDVI	1988	1997	2002	1986	1985	1995	2006
Precipitation	2007	2003	2007	1993	1991	2006	2004
Temperature	2007	1999	2000	1999	2000	1992	1985

significantly for alpine steppe, with the largest annual increase of 0.0017 year^{-1} ($R = 0.42$, $p = 0.02$) occurring in June and the lowest occurring in May (Figure 4(e), top). The trends in monthly climatic variables for all biome types, on the whole, showed warming and weak wetting trends at the beginning of the growing season, followed by significant warming and drying trends in the middle and at the end of the growing season, particularly for meadow steppe and typical steppe (Figure 4(b) and (c), middle and bottom), over the entire observation period. Intra-annual variations of NDVI and climatic variables for all biomes showed a similar pattern, with maximum values occurring in July or August.

Table 4 and Figure 5 show the TPs of monthly NDVI and climatic variables and their trends on both sides of the TPs. The detected TPs of monthly NDVI were not exactly coupled with climatic variables and varied strongly by month and by biome, with the earliest TP occurring in 1985 and the latest occurring in 2006. In comparison, the TPs of monthly NDVI for forest seem to have arrived earlier than for steppe grassland ecosystems generally.

From Figure 5, it can be clearly seen that opposite trends occurred on both sides of the TPs of all monthly NDVIs for all biomes. The monthly NDVIs for all biomes increased until the TP from May to October at a rate of 0.0003 year^{-1} (May, desert steppe) (Figure 5(d), top) to 0.0349 year^{-1} (June, meadow steppe) (Figure 5(b), top) and stalled or even decreased afterward at a rate of $-0.0055 \text{ year}^{-1}$ (May, meadow steppe) (Figure 5(b), top) to $-0.00001 \text{ year}^{-1}$ (September, alpine steppe) (Figure 5(e), top). An opposite phenomenon occurred in April, with a decreasing trend before the TP [$-0.0014 \text{ year}^{-1}$ for desert steppe (Figure 5(d), top) to $-0.0111 \text{ year}^{-1}$ for forest (Figure 5(a), top)] and a pronounced increasing trend after the TP [0.0007 year^{-1} for desert steppe (Figure 5(d), top) to 0.0028 year^{-1}

for meadow steppe (Figure 5(b), top)], suggesting that widespread vegetation greening (i.e. increasing NDVI) appears to dominate at the beginning of the growing season (April) after the TP. For forest, vegetation greening at the end of the growing season (September) was also very significant after the TP (Figure 5(a), top). At a monthly scale, the drying and warming climate appeared to dominate in summer months after the TP for most biomes.

3.4.2. Same-time response of monthly NDVI to climate change

To examine climate impacts on vegetation dynamics at a finer temporal scale, correlations between monthly NDVI and climatic variables were calculated during 1982–2010 (Table 5). For forest, the NDVI was correlated positively and significantly with temperature over all growing-season months except July, particularly for April ($R = 0.53$, $p = 0.003$), May ($R = 0.68$, $p < 0.0000$), June ($R = 0.48$, $p = 0.008$), and October ($R = 0.50$, $p = 0.005$). These results further confirmed the finding from previous studies that the large increase in NDVI over northern mid-to high latitudes can mainly be attributed to warming temperatures at the beginning and end of the growing season (Myneni *et al.*, 1997; Zhou *et al.*, 2001; Nemani *et al.*, 2003). However, it should also be noted that increasing temperature in the middle of the growing season (except for July) also plays a significant role in forest enhancement in Mongolia. An opposite relationship was found between forest NDVI and precipitation for all months except June ($R = 0.19$, $p = 0.34$), particularly in August ($R = -0.33$, $p = 0.08$), September ($R = -0.35$, $p = 0.06$), and October ($R = -0.38$, $p = 0.04$). This implies that perhaps precipitation in previous months, including snowfall during the winter, is preserved better in the soil of forest-dominated areas in Mongolia than elsewhere and that excessive

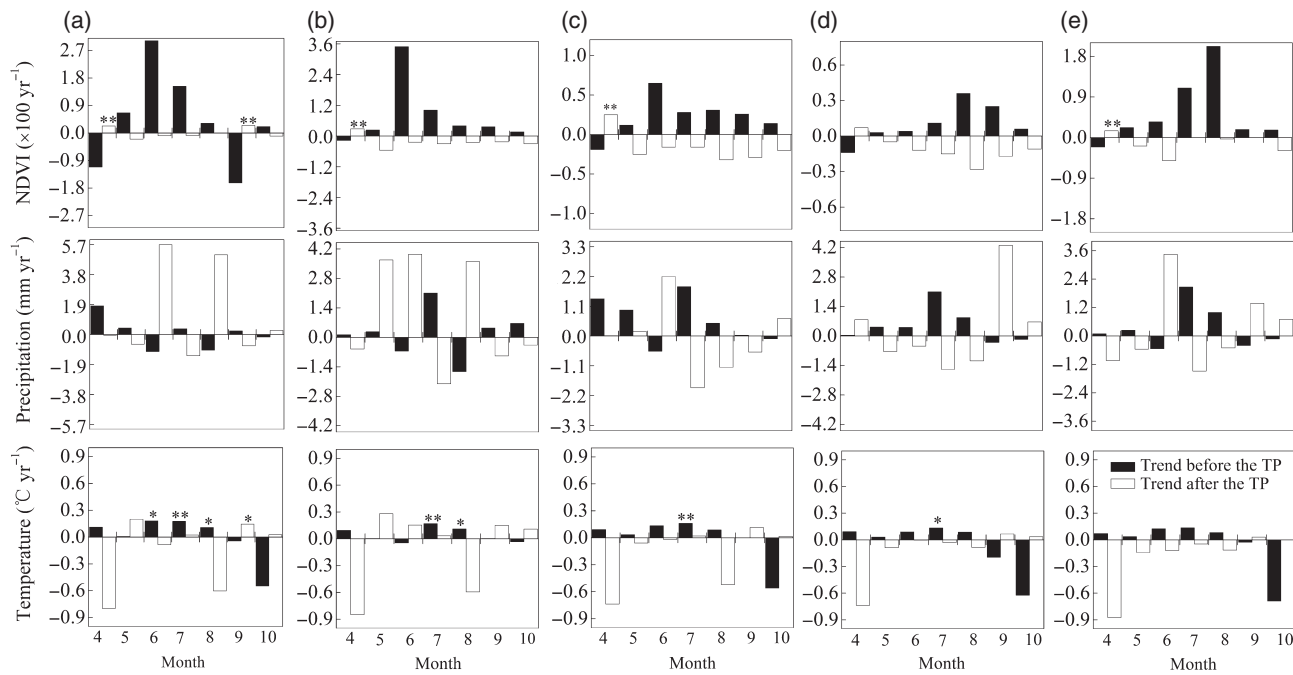


Figure 5. Dynamics of monthly NDVI and climatic variables from 1982 to 2010 for five biome types: (a) forest, (b) meadow steppe, (c) typical steppe, (d) desert steppe, and (e) alpine steppe.

Table 5. Correlation between monthly NDVI and corresponding climate variables for different biomes: monthly precipitation (P), monthly temperature (T).

Biome type	Climate variable	Correlation coefficient						
		April	May	June	July	August	September	October
Forest	P	−0.27	−0.03	0.19	−0.21	−0.33*	−0.35*	−0.38**
	T	0.53***	0.68***	0.48***	−0.04	0.32*	0.30	0.50***
Meadow steppe	P	0.04	0.16	0.22	0.43**	0.08	0.004	0.04
	T	0.24	0.38**	0.07	−0.37**	−0.31	0.13	0.25
Typical steppe	P	0.19	0.38**	0.43**	0.47***	0.39**	−0.03	0.05
	T	0.18	0.20	0.08	−0.44**	−0.43**	0.21	0.21
Desert steppe	P	−0.03	0.20	0.17	0.58***	0.52***	0.13	0.20
	T	−0.23	−0.07	0.07	−0.32*	−0.30	0.21	−0.21
Alpine steppe	P	−0.02	−0.41**	0.02	0.16	0.27	−0.24	−0.20
	T	0.37**	0.65***	0.67***	0.01	−0.13	0.28	0.31

***, **, and * indicate $p < 0.01$, $p < 0.05$, and $p < 0.1$, respectively.

rainfall could depress forest growth in the same month by reducing temperature and radiation, particularly in autumn months (Mao *et al.*, 2012). This can be further confirmed by the lagged time responses to climate change (Section 3.4.3). Alternatively, this effect might also arise from seasonally frozen ground in forest regions, which could provide adequate moisture during the growing season (Han *et al.*, 2014). Unlike that in forest ecosystems, NDVI for almost all growing-season months was, in general, positively correlated with precipitation for meadow steppe, typical steppe, and desert steppe and was related positively to temperature in the early and late growing season, but negatively and significantly in July (meadow: $R = -0.37$, $p = 0.05$; typical: $R = -0.44$, $p = 0.02$; desert: $R = -0.32$, $p = 0.10$) and August (meadow: $R = -0.31$, $p = 0.10$; typical: $R = -0.43$, $p = 0.02$; desert: $R = -0.30$, $p = 0.10$). However, the strength of the correlation differed markedly

among the different kinds of steppe. For example, the NDVI of meadow steppe was more closely related with temperature in May ($R = 0.38$, $p = 0.04$) than that of typical steppe ($R = 0.20$, $p = 0.30$) and desert steppe ($R = -0.07$, $p = 0.72$). In contrast, the NDVIs of typical steppe and desert steppe were more strongly correlated with precipitation than that of meadow steppe, particularly in July and August. There was also an opposite correlation between NDVI and temperature in April, May, and October for typical steppe ($R = 0.18$, $p = 0.36$; $R = 0.20$, $p = 0.30$; $R = 0.21$, $p = 0.26$) and desert steppe ($R = -0.23$, $p = 0.24$; $R = -0.07$, $p = 0.72$; $R = -0.21$, $p = 0.27$).

These discrepancies in the response to monthly climate variables among the various kinds of steppe could be associated with their different climatic growth environments, as represented by factors such as moisture index and thermal condition. Figure 6 shows the variation of

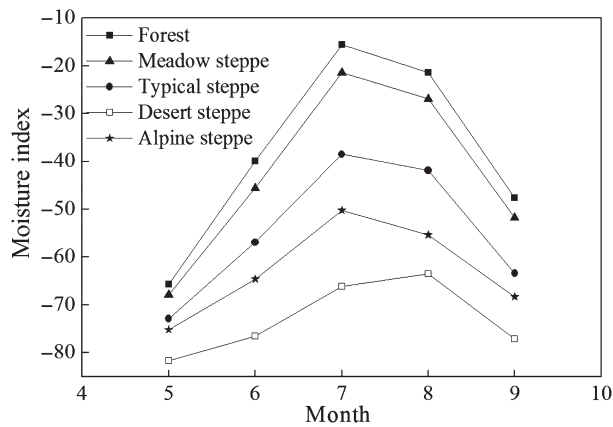


Figure 6. Variation of multi-year mean monthly moisture index by biome.

Thornthwaite's moisture index (Thornthwaite, 1948) for different biome types. From meadow steppe to typical steppe and then to desert steppe, the moisture index decreased for all growing-season months, with the largest differences in July and August (Figure 6). Therefore, the relationship between monthly NDVI and precipitation became stronger as the moisture index decreased from meadow steppe to typical steppe and then to desert steppe, particularly in July and August, because the largest difference in moisture index occurred in July and August. In contrast, meadow steppe in Mongolia is generally distributed under conditions with more moisture and lower temperature than those of typical and desert steppe, and therefore there was a stronger positive correlation with temperature in May than for typical and desert steppe. However, the negative impact of temperature on meadow steppe vegetation growth in July and August was still more significant in Mongolia (Table 5), implying that vegetation growth of meadow steppe in Mongolia is strongly hindered by rising temperature-induced drought conditions in mid- and late summer. This phenomenon is inconsistent with that observed in temperate meadow in China by Piao, who suggested a positive correlation between meadow NDVI and temperature in summer (Piao *et al.*, 2006b). For alpine steppe, the monthly NDVI was significantly and positively related to temperature in April ($R = 0.37$, $p = 0.05$), May ($R = 0.65$, $p = 0.0001$), and June ($R = 0.67$, $p < 0.0000$), but negatively to precipitation in May ($R = -0.41$, $p = 0.03$) (Table 5), indicating that temperature in the early growing season and in early summer (June) has a strong positive influence on alpine steppe vegetation growth in Mongolia. The negative correlation with precipitation was not consistent with the results for alpine meadow on the Tibetan Plateau reported by Piao, where positive correlations were observed (Piao *et al.*, 2006a).

3.4.3. Lagged time response of monthly NDVI to climate change

Even as climate factors change, vegetation growth takes time to respond, and time lags most likely vary for different

climate factors and different areas (Braswell *et al.*, 1997; Hu *et al.*, 2011) because of delays in the adjustment of soil moisture content and biological processes (Davenport and Nicholson, 1993). Figure 7 shows the correlation coefficients between monthly NDVI and climatic variables in all previous months for each biome type during 1982–2010. The lag period and the strength of the lag effect of climate varied by biome and by month. For forest, significant positive correlations were found between NDVI in April ($R = 0.33$, $p = 0.08$), May ($R = 0.33$, $p = 0.08$), and September ($R = 0.44$, $p = 0.02$) and temperature from the preceding month (Figure 7(a)), implying that there exists a 1-month lag effect of temperature on forest NDVI in the early growing season and in late summer (August). However, the strength of this relationship was much less than that of the relationship with no time lag (Table 5), suggesting that temperature conditions in the same month may be more critically important to forest growth at the beginning and end of the growing season in Mongolia. Unlike the negative effect of precipitation on NDVI in the same month, there was always a positive precipitation lag effect on forest NDVI except in May, September, and October (Figure 7(b)). This may have been the reason for a significant negative correlation between NDVI and precipitation in the same month (Table 5), because precipitation from the preceding month could maintain enough moisture in the deeper-rooted forest system, in which case precipitation in the same month may lead to surplus water, thereby depressing forest growth.

Similarly to forest, almost all NDVI values for meadow steppe, typical steppe, and desert steppe in April, May, and October were positively but weakly correlated with temperature in the preceding month (Figure 7(c), (e), and (g)), indicating that higher temperatures in the preceding month could favour grass growth at the beginning and end of the growing season. However, temperatures in May, June, July, and August had about a 1- to 3-month lagged negative effect on grass growth. A similar trend was observed in the whole of China by Piao, who demonstrated an approximately 3-month lag effect of temperature on vegetation (Piao *et al.*, 2003). However, the positive lagged effect of precipitation on the three steppe types was more significant, and the period of the lag varied by month (Figure 7(d), (f), and (h)). Generally, there is a 1-month lag effect on vegetation response to precipitation in March, April, and May and a 1- to 4-month lag effect from precipitation in June, July, and August, suggesting that spring and summer precipitation is a key factor for annual vegetation growth in Mongolia, particularly for grass growth in the middle and at the end of the growing season. This long-term effect of precipitation in summer on grass growth in Mongolia is longer than that observed by Shinoda in dry savannas in Africa, where there existed at most a 2.5-month lag effect (Shinoda, 1995). In addition, almost all the lag effects of precipitation are stronger than that with no time lag (Table 5), suggesting the importance of antecedent precipitation conditions for grass growth. For alpine grassland, temperature

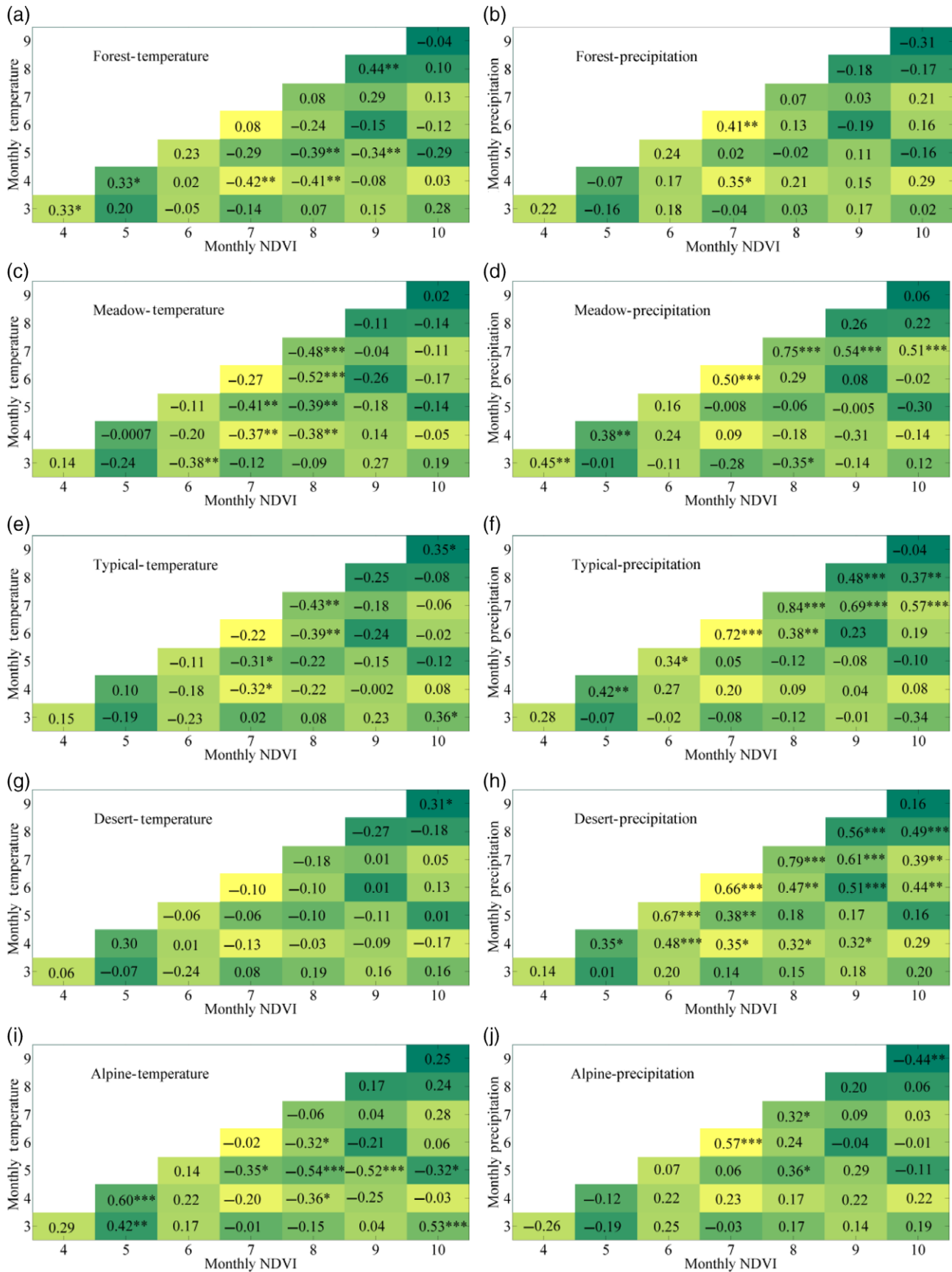


Figure 7. Correlation between monthly NDVI and climatic variables from all previous months by biome during 1982–2010. ***, **, and * indicate $p < 0.01$, $p < 0.05$, and $p < 0.1$, respectively.

for March, April, May, August, and September shows a positive relationship with NDVI in the subsequent 1 or 2 months (Figure 7(i)), indicating that rising temperature during these months is favourable for alpine grass growth, particularly temperature in March and April, whereas an opposite trend was observed in the correlations between NDVI in July and August and the two climatic variables from preceding months.

4. Conclusions

In this study, a monthly NDVI sequence has been developed for Mongolia covering the period 1982–2010 by calibrating the MODIS NDVI (2000–2010) to the GIMMS NDVI (1982–2006) based on the overlapping period of 2000–2006. The calibration results from pixel-based models demonstrated that the continuity and consistency of the newly constructed NDVI are in acceptable agreement with the GIMMS NDVI for each biome and can detect subtle trends in the long-term vegetation dynamics of Mongolia. Based on these NDVI datasets and climatic variables (temperature and precipitation) from 1982 to 2010, the growing-season and monthly vegetation dynamics for five biomes and their response to regional climate change have been thoroughly investigated. The results show that vegetation growth for all biomes in Mongolia reversed (from an increasing to a decreasing trend) between 1991 and 1994 and that desertification is becoming one of the most significant ecological stresses in Mongolia for most biomes, particularly for meadow steppe, typical steppe, and desert steppe. This TP of vegetation growth trend in Mongolia was about 3–6 years earlier than in the rest of Eurasia. Pronounced drying trends occurring between 1990 and 1994 and a persistently warming climate until recently have likely played a major role in the NDVI trend reversal. However, the timing of the NDVI trend reversal (TP year) at both growing-seasonal scale and monthly scale was not exactly coupled with the TP of either precipitation or temperature, implying a nonlinear response of trend reversal in vegetation growth to any single climatic variable. On a long-term scale, the impacts of climate change on vegetation growth varied greatly among different biomes, months, and climates due to differences in growth environments and their corresponding climatic regimes. Generally, growing-season NDVI was positively related to temperature and negatively to precipitation for forest, and opposite trends in the correlations between NDVI and temperature and NDVI and precipitation were observed in steppe grassland ecosystems. In addition, this study also shows that the long-time lag effects of climatic variables on vegetation growth are different in different biomes, mostly varying from 1- to 4-month lags, and also vary by climatic variable and by month. This study will be significant for improving our understanding of ecological evolution and highlighting early signs for prevention of natural hazards like desertification and sandstorms in Mongolia and other surrounding East Asian regions such as North China and Korea.

Acknowledgements

This study was supported by the National Natural Science Foundation of China (grant no: 41301456), the national ‘twelve-five’ Technology Support Project of China (grant no: 2013BAK05B01), the National Basic Research Program of China (973 Program) (grant no: 2010CB951504), and the International Science and Technology Cooperation Project of China (2012DFA31290). We would like to thank the anonymous reviewers for providing constructive suggestions and also to thank the MODIS and AVHRR science teams for providing accessible data products.

References

- Braswell B, Schimel D, Linder E, Moore B. 1997. The response of global terrestrial ecosystems to interannual temperature variability. *Science* **278**(5339): 870–873, doi: 10.1126/science.278.5339.870.
- Brown ME, Lary DJ, Vrieling A, Stathakis D, Mussa H. 2008. Neural networks as a tool for constructing continuous NDVI time series from AVHRR and MODIS. *Int. J. Remote Sens.* **29**(24): 7141–7158, doi: 10.1080/01431160802238435.
- Chen B, Xu G, Coops NC, Ciais P, Innes JL, Wang G, Myneni RB, Wang T, Krzyzanowski J, Li Q. 2014. Changes in vegetation photosynthetic activity trends across the Asia-Pacific region over the last three decades. *Remote Sens. Environ.* **144**: 28–41, doi: 10.1016/j.rse.2013.12.018.
- Chuai XW, Huang XJ, Wang WJ, Bao G. 2013. NDVI, temperature, and precipitation changes and their relationships with different vegetation types during 1998–2007 in Inner Mongolia, China. *Int. J. Climatol.* **33**(7): 1696–1706, doi: 10.1002/joc.3543.
- Davenport M, Nicholson S. 1993. On the relation between rainfall and the normalized difference vegetation index for diverse vegetation types in East Africa. *Int. J. Remote Sens.* **14**(12): 2369–2389, doi: 10.1080/01431169308954042.
- Eastman JR, Sangermano F, Machado EA, Rogan J, Anyamba A. 2013. Global trends in seasonality of normalized difference vegetation index (NDVI), 1982–2011. *Remote Sens.* **5**(10): 4799–4818, doi: 10.3390/rs5104799.
- Eckert S, Hüsler F, Liniger H, Hodel E. 2015. Trend analysis of MODIS NDVI time series for detecting land degradation and regeneration in Mongolia. *J. Arid Environ.* **113**: 16–28.
- Fensholt R, Proud SR. 2012. Evaluation of Earth observation-based global long-term vegetation trends – comparing GIMMS and MODIS global NDVI time series. *Remote Sens. Environ.* **119**: 131–147, doi: 10.1016/j.rse.2009.04.004.
- Fensholt R, Rasmussen K, Nielsen TT, Mbow C. 2009. Evaluation of Earth observation-based long-term vegetation trends – intercomparing NDVI time series trend analysis consistency of Sahel from AVHRR GIMMS, Terra MODIS, and SPOT VGT data. *Remote Sens. Environ.* **113**: 1886–1898, doi: 10.1016/j.rse.2009.04.004.
- Fernandez-Gimenez M, Allen-Diaz B. 2001. Vegetation change along gradients from water sources in three grazed Mongolian ecosystems. *Plant Ecol.* **157**(1): 101–118, doi: 10.1023/A:1014519206041.
- Fujiwara H, Fukuyama T, Shirato Y, Ohkuro T, Taniyama I, Zhang TH. 2007. Deposition of atmospheric ¹³⁷Cs in Japan associated with the Asian dust event of March 2002. *Sci. Total Environ.* **384**(1–3): 306–315, doi: 10.1016/j.scitotenv.2007.05.024.
- Han L, Tsunekawa A, Tsubo M, He C, Shen M. 2014. Spatial variations in snow cover and seasonally frozen ground over northern China and Mongolia, 1988–2010. *Glob. Planet. Change* **116**: 139–148, doi: 10.1016/j.gloplacha.2014.02.008.
- Hoffmann WA, Jackson RB. 2000. Vegetation-climate feedbacks in the conversion of tropical savanna to grassland. *J. Clim.* **13**(9): 1593–1602, doi: 10.1175/1520-0442(2000)013<1593:VCFITC>2.0.CO;2.
- Holben BN. 1986. Characteristics of maximum-value composite images from temporal AVHRR data. *Int. J. Remote Sens.* **7**(11): 1417–1434, doi: 10.1080/01431168608948945.
- Hu MQ, Mao F, Sun H, Hou YY. 2011. Study of normalized difference vegetation index variation and its correlation with climate factors in the three-river source region. *Int. J. Appl. Earth Obs. Geoinf.* **13**(1): 24–33, doi: 10.1016/j.jag.2010.06.003.

- Huete AR. 1988. A soil-adjusted vegetation index (SAVI). *Remote Sens. Environ.* **25**(3): 295–309, doi: 10.1016/0034-4257(88)90106-X.
- Huete AR, Didan K, Miura T, Rodriguez EP, Gap X, Ferreira LG. 2002. Overview of the radiometric and biophysical performance of the MODIS vegetation indices. *Remote Sens. Environ.* **83**: 195–213.
- Huntley BJ, Webb T. 1988. *Vegetation History*. Kluwer: Dordrecht, The Netherlands.
- Ichii K, Kawabata A, Yamaguchi Y. 2002. Global correlation analysis for NDVI and climatic variables and NDVI trends: 1982–1990. *Int. J. Remote Sens.* **23**(18): 3873–3878, doi: 10.1080/01431160110119416.
- Jiang DJ, Fu XF, Wang K. 2013. Vegetation dynamics and their response to freshwater inflow and climate variables in the Yellow River Delta, China. *Quat. Int.* **304**: 75–84, doi: 10.1016/j.quaint.2012.10.059.
- Li X, Cheng GD, Lu L. 2005. Spatial analysis of air temperature in the Qinghai-Tibet Plateau. *Arct. Antarct. Alp. Res.* **37**(2): 246–252.
- Li SG, Eugster W, Asanuma J, Kotani A, Davaa G, Oyunbaatar D, Sugita M. 2008. Response of gross ecosystem productivity, light use efficiency, and water use efficiency of Mongolian steppe to seasonal variations in soil moisture. *J. Geophys. Res.* **113**(G1): G01019, doi: 10.1029/2006JG000349.
- Lu Y, Zhuang Q, Zhou G, Sirin A, Melillo J, Kicklighter D. 2009. Possible decline of the carbon sink in the Mongolian Plateau during the 21st century. *Environ. Res. Lett.* **4**(4): 045023, doi: 10.1088/1748-9326/4/4/045023.
- Mao DH, Wang ZM, Luo L, Ren CY. 2012. Integrating AVHRR and MODIS data to monitor NDVI changes and their relationships with climatic parameters in Northeast China. *Int. J. Appl. Earth Obs. Geoinf.* **18**: 528–536, doi: 10.1007/s11442-013-1062-2.
- Myneni RB, Keeling C, Tucker C, Asrar G, Nemani RR. 1997. Increased plant growth in the northern high latitudes from 1981 to 1991. *Nature* **386**(6626): 698–702, doi: 10.1038/386698a0.
- National Statistical Office of Mongolia. 2011. *Mongolian Statistical Yearbook*. National Statistical Office of Mongolia: Ulaanbaatar, 19–20.
- Nemani RR, Keeling CD, Hashimoto H, Jolly WM, Piper SC, Tucker CJ, Myneni RB, Running SW. 2003. Climate-driven increases in global terrestrial net primary production from 1982 to 1999. *Science* **300**(5625): 1560–1563, doi: 10.1126/science.1082750.
- Neupert RF. 1999. Population, nomadic pastoralism, and the environment in the Mongolian Plateau. *Popul. Environ.* **20**(5): 413–441.
- Park HS, Sohn B. 2010. Recent trends in changes of vegetation over East Asia coupled with temperature and rainfall variations. *J. Geophys. Res. Atmos.* **115**: D14101, doi: 10.1029/2009JD012752.
- Piao SL, Fang JY, Zhou LM, Guo QH, Henderson M, Ji W, Li Y, Tao S. 2003. Interannual variations of monthly and seasonal normalized difference vegetation index (NDVI) in China from 1982 to 1999. *J. Geophys. Res.* **108**(D14): 4401, doi: 10.1029/2002JD002848.
- Piao SL, Fang JY, He JS. 2006a. Variations in vegetation net primary production in the Qinghai-Xizang Plateau, China, from 1982 to 1999. *Clim. Change* **74**(1–3): 253–267, doi: 10.1007/s10584-005-6339-8.
- Piao SL, Mohammad A, Fang JY, Cai Q, Feng JM. 2006b. NDVI-based increase in growth of temperate grasslands and its responses to climate changes in China. *Glob. Environ. Change* **16**(4): 340–348, doi: 10.1016/j.gloenvcha.2006.02.002.
- Piao SL, Wang XH, Ciais P, Zhu B, Wang T, Liu J. 2011. Changes in satellite-derived vegetation growth trend in temperate and boreal Eurasia from 1982 to 2006. *Glob. Change Biol.* **17**(10): 3228–3239, doi: 10.1111/j.1365-2486.2011.02419.x.
- Potter C, Boriah S, Steinbach M, Kumar V, Klooster S. 2008. Terrestrial vegetation dynamics and global climate controls. *Clim. Dyn.* **31**(1): 67–78, doi: 10.1007/s00382-007-0339-5.
- Rocchini D. 2007. Effects of spatial and spectral resolution in estimating ecosystem α -diversity by satellite imagery. *Remote Sens. Environ.* **111**(4): 423–434, doi: 10.1016/j.rse.2007.03.018.
- Ruse JW, Haas RH, Schell JA, Deering DW, Harlan JC. 1974. Monitoring the vernal advancements and retrogradation of natural vegetation. Final Report, NASA/GSFC, Greenbelt, MD, 1–137.
- Schmidt M, Klein D, Conrad C, Dech S, Paeth H. 2014. On the relationship between vegetation and climate in tropical and northern Africa. *Theor. Appl. Climatol.* **115**(1–2): 341–353, doi: 10.1007/s00704-013-0900-6.
- Serreze M, Walsh J, Chapin IF, Osterkamp T, Dyurgerov M, Romanovsky V, Oechel W, Morison J, Zhang T, Parry R. 2000. Observational evidence of recent change in the northern high-latitude environment. *Clim. Change* **46**(1–2): 159–207, doi: 10.1023/A:1005504031923.
- Shinoda M. 1995. Seasonal phase lag between rainfall and vegetation activity in tropical Africa as revealed by NOAA satellite data. *Int. J. Climatol.* **15**(6): 639–656, doi: 10.1002/joc.3370150605.
- Steven MD, Malthus TJ, Baret F, Xu H, Chopping MJ. 2003. Inter-calibration of vegetation indices from different sensor systems. *Remote Sens. Environ.* **88**(4): 412–422, doi: 10.1016/j.rse.2003.08.010.
- Thornthwaite CW. 1948. An approach toward a rational classification of climate. *Geogr. Rev.* **38**: 55–94.
- Tomé A, Miranda P. 2004. Piecewise linear fitting and trend changing points of climate parameters. *Geophys. Res. Lett.* **31**(2): L02207, doi: 10.1029/2003GL019100.
- Toms JD, Lesperance ML. 2003. Piecewise regression: a tool for identifying ecological thresholds. *Ecology* **84**(8): 2034–2041.
- Tucker CJ, Slayback DA, Pinzon JE, Los SO, Myneni RB, Taylor MG. 2001. Higher northern latitude normalized difference vegetation index and growing season trends from 1982 to 1999. *Int. J. Biometeorol.* **45**(4): 184–190, doi: 10.1007/s00484-001-0109-8.
- Upton C. 2010. Living off the land: nature and nomadism in Mongolia. *Geoforum* **41**: 865–874.
- Walther GR, Post E, Convey P, Menzel A, Parmesan C, Beebee TJ, Fromentin JM, Guldberg H, Bairlein F. 2002. Ecological responses to recent climate change. *Nature* **416**(6879): 389–395, doi: 10.1038/416389a.
- Wang XH, Piao SL, Ciais P, Li JS, Friedlingstein P, Koven C, Chen AP. 2011. Spring temperature change and its implication in the change of vegetation growth in North America from 1982 to 2006. *Proc. Natl. Acad. Sci. U.S.A.* **108**(4): 1240–1245, doi: 10.1073/pnas.1014425108.
- Watson RT, Albritton DL. 2001. *Climate Change 2001: Synthesis Report*. Cambridge University Press: Cambridge, UK.
- Whitlock C, Bartlein PJ. 1997. Vegetation and climate change in north-west America during the past 125 kyr. *Nature* **388**(6637): 57–61, doi: 10.1038/40380.
- Wu TT, Li YR. 2013. Spatial interpolation of temperature in the United States using residual kriging. *Appl. Geogr.* **44**: 112–120.
- Yao J, He XY, Li XY, Chen W, Tao DL. 2012. Monitoring responses of forest to climate variations by MODIS NDVI: a case study of Hun River upstream, northeastern China. *Eur. J. For. Res.* **131**(3): 705–716, doi: 10.1007/s10342-011-0543-z.
- Zemlich A, Manthey M, Zerbe S, Oyunchimeg D. 2010. Driving environmental factors and the role of grazing in grassland communities: a comparative study along an altitudinal gradient in Western Mongolia. *J. Arid Environ.* **74**(10): 1271–1280, doi: 10.1016/j.jaridenv.2010.05.014.
- Zhang XY, Hu YF, Zhuang DF, Qi YQ, Ma X. 2009. NDVI spatial pattern and its differentiation on the Mongolian Plateau. *J. Geogr. Sci.* **19**(4): 403–415.
- Zhang YL, Gao JG, Liu LS, Wang ZF, Ding MJ, Yang XC. 2013. NDVI-based vegetation changes and their responses to climate change from 1982 to 2011: a case study in the Koshi River Basin in the middle Himalayas. *Glob. Planet. Change* **108**(2013): 139–148, doi: 10.1016/j.gloplacha.2013.06.012.
- Zhou LM, Tucker CJ, Kaufmann RK, Slayback D, Shabanov NV, Myneni RB. 2001. Variations in northern vegetation activity inferred from satellite data of vegetation index during 1981 to 1999. *J. Geophys. Res. Atmos.* **106**(D17): 20069–20083, doi: 10.1029/2000JD000115.
- Zou XK, Zhai PM. 2004. Relationship between vegetation coverage and spring dust storms over northern China. *J. Geophys. Res. Atmos.* **109**: D03104, doi: 10.1029/2003JD003913.

NDVI-indicated long-term vegetation dynamics in Mongolia and their response to climate change at biome scale

Gang Bao,^{a,b} Yuhai Bao,^{a*} Amarjargal Sanjjava,^c Zhihao Qin,^{b,d} Yi Zhou^b and Guang Xu^{e,f}

^a Inner Mongolia Key Laboratory of Remote Sensing and Geographic Information Systems, Inner Mongolia Normal University, Hohhot, China

^b International Institute for Earth System Science, Nanjing University, China

^c Institute of Geography, Mongolian Academy of Science, Ulaanbaatar, Mongolia

^d Institute of Agro-Resources and Regional Planning, Chinese Academy of Agricultural Sciences, Beijing, China

^e Institute of Geographic Sciences and Natural Resources Research, Chinese Academy of Sciences, Beijing, China

^f University of Chinese Academy of Sciences, Beijing, China

ABSTRACT: Based on the vegetation map of Mongolia, Global Inventory Monitoring and Modelling Studies (GIMMS) normalized difference vegetation index (NDVI) (1982–2006), the Moderate Resolution Imaging Spectroradiometer (MODIS) NDVI (2000–2010), and temperature and precipitation data derived from 60 meteorological stations, this study has thoroughly examined vegetation dynamics in Mongolia and their responses to regional climate change at biome scale. To ensure continuity and consistency between the two NDVI datasets, the MODIS NDVI was first calibrated to the GIMMS NDVI based on the overlapping period of 2000–2006. Good calibration results with R^2 values of 0.86–0.98 between the two NDVI datasets were obtained and can detect subtle trends in the long-term vegetation dynamics of Mongolia. The results indicated that for various biomes, although NDVI changes during 1982–2010 showed great variation, vegetation greening for all biomes in Mongolia seem to have stalled or even decreased since 1991–1994, particularly for meadow steppe (0.0015 year^{-1}), typical steppe ($-0.0010 \text{ year}^{-1}$), and desert steppe ($-0.0008 \text{ year}^{-1}$), which is an apparent turning point (TP) of the vegetation growth trend in Mongolia. A pronounced drying trend (from $-4.399 \text{ mm year}^{-1}$ in meadow steppe since 1990 to $-2.445 \text{ mm year}^{-1}$ in alpine steppe since 1993) occurred between 1990 and 1994, and persistently warming temperatures ($0.015 \text{ }^{\circ}\text{C year}^{-1}$ in alpine steppe to $0.070 \text{ }^{\circ}\text{C year}^{-1}$ in forest and meadow steppe) until recently have likely played a major role in this NDVI trend reversal. However, the NDVI TP varied by biome, month, and climate and was not coupled exactly with climatic variables. The impact on climate of both same-time and lagged-time temperature and precipitation effects also varied strongly across biomes and months. On the whole, climate-related vegetation decline and associated potential desertification trends will likely be among the major sources of ecological pressure for each biome in Mongolia, which could intensify environmental problems like sandstorms in other East Asian regions.

KEY WORDS climate change; vegetation dynamics; NDVI; Mongolia; biome scale

Received 10 August 2014; Revised 2 January 2015; Accepted 16 January 2015

1. Introduction

Vegetation not only serves as a direct indicator of the status of terrestrial ecosystems as well as local and global environmental changes (Potter *et al.*, 2008; Jiang *et al.*, 2013) but also regulates the carbon cycle, energy exchange, and climate change in the Earth's systems in direct and indirect ways, including photosynthesis, surface albedo, evapotranspiration, and roughness (Wang *et al.*, 2011; Chen *et al.*, 2014). Regional vegetation history is generally regarded as a footprint of climate variations and provides an excellent opportunity to examine climate change impacts on ecosystems through time, space, or both (Huntley and Webb, 1988; Whitlock and Bartlein, 1997). Therefore, vegetation dynamics and their response to global climate change (focusing mostly on precipitation

and temperature) have increasingly become a main focus of global change studies, particularly since the 1980s when the satellite-derived normalized difference vegetation index (NDVI) became available (Myneni *et al.*, 1997; Tucker *et al.*, 2001; Zhou *et al.*, 2001; Nemani *et al.*, 2003; Potter *et al.*, 2008; Piao *et al.*, 2011; Wang *et al.*, 2011; Chen *et al.*, 2014). Most of these studies have generally suggested that vegetation photosynthetic activity (NDVI) in northern high latitudes increased from the 1980s to the 1990s with increases in temperature (Myneni *et al.*, 1997; Tucker *et al.*, 2001; Zhou *et al.*, 2001; Nemani *et al.*, 2003; Piao *et al.*, 2006a). However, studies on continental or global scales may neglect small-scale heterogeneity to some extent if national or local heterogeneity has not had a decisive effect on continental or global vegetation dynamics because these studies miss a certain amount of local detail due to the coarse spatial resolution of Global Inventory Monitoring and Modelling Studies (GIMMS) NDVI data and differences in observation period (Walther *et al.*, 2002; Rocchini, 2007; Yao *et al.*, 2012). In addition,

* Correspondence to: Y. Bao, Inner Mongolia Key Laboratory of Remote Sensing and Geographic Information Systems, Inner Mongolia Normal University, Hohhot, China. E-mail: baoyuhai@imnu.edu.cn

vegetation dynamics and their responses to climate change have varied considerably due to different ecogeographical conditions (Chuai *et al.*, 2013), and therefore examining the effect of climate on vegetation dynamics at the biome scale, particularly at finer temporal scales (such as monthly or even shorter timescales), could gain further insight into the mechanisms of interaction between climate and vegetation variability (Chen *et al.*, 2014).

The Republic of Mongolia lies in a transitional zone from the Gobi Desert of central Asia in the southwest to the Siberian taiga forest in the north (Li *et al.*, 2008). Most of the Mongolian territory is characterized by arid and semiarid climate, and over 70% of Mongolia is covered by high-quality steppe grasslands (Fernandez-Gimenez and Allen-Diaz, 2001) with high sensitivity to global climate change (Watson and Albritton, 2001). As in other (semi)arid regions, although precipitation is the primary climatic control on vegetation activity at a national scale (Myneni *et al.*, 1997; Zhou *et al.*, 2001; Zemmrich *et al.*, 2010) and may even overcome the negative effects of grazing intensity (Zemmrich *et al.*, 2010), the relatively complex contribution of vegetation-related climatic variables to vegetation dynamics may be regionally dependent and may vary strongly by biome. Therefore, it is hypothesized here that vegetation dynamics, particularly at biome scales, and their response to climate change in Mongolia may not be completely consistent with the results of studies conducted in areas where temperature is a more important factor in plant growth. Furthermore, compared to other regions in northern high latitudes, the intensity of climate warming in Mongolia has tended to be greater than the global average (Serreze *et al.*, 2000; Lu *et al.*, 2009). This would severely aggravate drought stress without a concurrent increase in rainfall, restricting plant growth and even intensifying desertification tendencies and other related disasters like sandstorms and soil erosion (Zou and Zhai, 2004). In addition, the population of Mongolia was 2.83 million in 2011, with the lowest density in the world, 1.8 persons per square kilometre (National Statistical Office of Mongolia, 2011), and nomadic herding has been the predominant Mongolian economic activity from ancient times until now (Neupert, 1999). This situation leads to minimal human impact on the ecosystem and recommends Mongolia as an ideal region for exploring the mechanisms of interaction between climate change and vegetation dynamics. However, very few studies (Zhang *et al.*, 2009; Eckert *et al.*, 2015) on nation-scale vegetation dynamics in Mongolia have been performed over the past three decades, despite the ecological and geographical significance of Mongolia, such as its role as a birthplace of sandstorms (Fujiwara *et al.*, 2007).

One of the common ways to explore vegetation changes and their response to climate change is to use the satellite-derived NDVI (Myneni *et al.*, 1997; Nemani *et al.*, 2003; Chen *et al.*, 2014) because NDVI is highly correlated with photosynthetically active biomass, leaf area, chlorophyll abundance, and potential photosynthesis of vegetation (Nemani *et al.*, 2003; Schmidt *et al.*, 2014). It is based on the contrast between the

absorption in the red band due to vegetation chlorophyll pigments and the reflection in the infrared band caused by leaf cellular structure and is calculated as $NDVI = (NIR - RED) / (NIR + RED)$, where RED and NIR represent the reflectance in the red and near-infrared band, respectively (Ruse *et al.*, 1974). Although NDVI has several limitations, including saturation in a densely vegetated canopy and an intensively noisy canopy background signal in sparsely vegetated regions (Huete *et al.*, 2002), it is widely used in vegetation dynamics studies from local to global scales after processing to monthly maximum composite values, which can greatly reduce noise (Nemani *et al.*, 2003; Zhang *et al.*, 2013), particularly in northern latitudes (Myneni *et al.*, 1997; Tucker *et al.*, 2001). At present, although a number of NDVI datasets such as GIMMS NDVI (three generations), MODIS NDVI, and SPOT VGT NDVI have become available, no single NDVI time series covers the past three decades at large spatial extent except for GIMMS NDVI3g (Eastman *et al.*, 2013; Chen *et al.*, 2014). Therefore, there is a great need to combine the new NDVI time-series dataset from MODIS with the traditional GIMMS NDVI by developing a cross-calibration method between different NDVI datasets from different sensors (Steven *et al.*, 2003; Mao *et al.*, 2012). This would make it possible to extend vegetation dynamics measurements through time, particularly for future measurements, although GIMMS NDVI3g has become available recently (Eastman *et al.*, 2013; Chen *et al.*, 2014).

The objectives of the present study are (1) to develop an NDVI time series for the Mongolian ecosystem covering 1982–2010 by calibrating the MODIS NDVI (2000–2010) to the GIMMS NDVI (1982–2006) based on the overlapping period of 2000–2006; (2) to investigate what vegetation dynamics have occurred over the past 29 years at biome scales, and for what reasons, using a least-squares linear regression model (Zhou *et al.*, 2001) and a piecewise regression approach (Chen *et al.*, 2014); and (3) to examine NDVI variations and the turning point (TP) of NDVI trends for each month to detect the contribution of monthly NDVI to growing-season NDVI, and also to examine the monthly lagged impacts of climatic variables on vegetation dynamics at a biome scale, based on the vegetation map of Mongolia.

2. Data and methods

2.1. Study area

Mongolia is located in the heart of central Asia and stretches from approximately 41°–52°N and 81°–119°E, with an area of approximately 156×10^4 km² (Figure 1). The climatic regime is characterized by a typical continental climate, with annual precipitation ranging between 50 mm in the southwestern Gobi Desert area and 350 mm in the northern forested region. The temperature gradient slopes in the opposite sense to that of precipitation, ranging from less than 1.5 °C in the northern mountains to over 16 °C in the southwestern Gobi Desert. Mongolia has

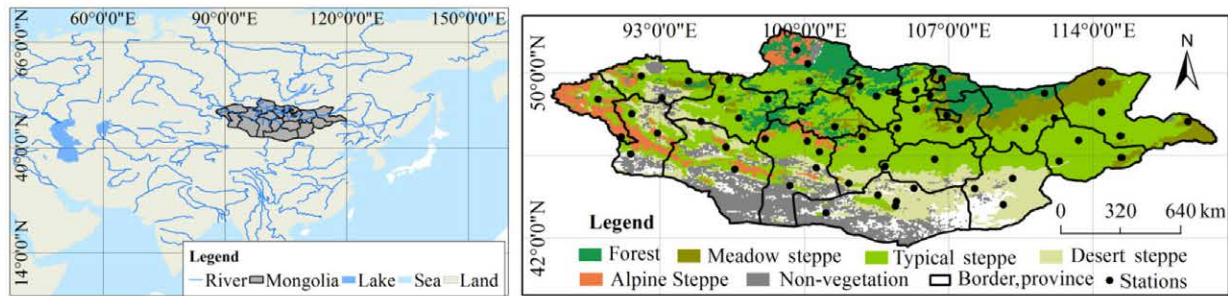


Figure 1. Location of study area and distribution of biomes and meteorological stations.

one of the largest undeveloped grassland ecosystems in the world (Lu *et al.*, 2009) except for the northern forested area and the southwestern Gobi Desert, and all these ecosystems are very sensitive to climate change (Li *et al.*, 2008). Under the influence of climatic differentiation, vegetation across Mongolia displays an obvious latitudinal zonation, passing through forest, meadow steppe, typical steppe, desert steppe, and the Gobi Desert from north to south and from northeast to southwest. Alpine steppe is also distributed in the northern and western mountain ranges (Figure 1).

2.2. Dataset

NDVI datasets produced by the GIMMS group using the Advanced Very High Resolution Radiometer (AVHRR)/the National Oceanic and Atmospheric Administration (NOAA) series satellites (NOAA 7, 9, 11, 14, 16, 17, and 18) and the MOD12C1 NDVI product (Level-3 product) derived from the Terra MODIS instrument were used in the present study. The GIMMS NDVI covers the period from 1982 to 2006 and has a resolution of 8 km and an interval of 15 days, whereas the MODIS NDVI covers the period from 2000 to 2010 and has a resolution of 5.6 km and an interval of 16 days. These two NDVI datasets have been corrected to remove noise from solar angle and sensor errors and have been widely used in studies on monitoring of long-term vegetation activity from regional to global scales (Nemani *et al.*, 2003; Mao *et al.*, 2012). To decrease some non-vegetation effects further, a monthly NDVI dataset was generated for both GIMMS and MODIS NDVI by applying the maximum value composite (MVC) method (Holben, 1986) to the two NDVI images for each growing-season month. To match the spatial resolution of the GIMMS NDVI, the MODIS NDVI was then further spatially resampled to 8 km. The growing season was defined as from April to October, and growing-season NDVI data were obtained by averaging monthly NDVI data from April to October for each year (Piao *et al.*, 2011). The growing-season average NDVI can phenologically be regarded as the average measurable level of photosynthetic activity during 1 year (Chen *et al.*, 2014), which is a meaningful indicator of interannual vegetation dynamics at regional scale (Chuai *et al.*, 2013).

The climate variables used were the growing-season monthly precipitation amount and the mean temperature derived from 60 meteorological stations across Mongolia,

as provided by the Mongolian Weather Bureau and the Institute of Geography, Mongolian Academy of Science. According to the locations of the meteorological stations, monthly climatic data were interpolated in the ArcGIS environment using the kriging method at a spatial resolution of 8 km to match both temporally and spatially the time sequences of growing-season mean NDVI. Although some errors may have resulted from the areal interpolation due to the limited number of meteorological stations available (Piao *et al.*, 2003), previous studies have demonstrated that kriging is a better interpolation method with higher accuracy and lower bias than other methods (Li *et al.*, 2005; Wu and Li, 2013), particularly in areas with uniformly distributed climate stations (Figure 1) and having minimal elevation changes and subdued topography (mostly grassland ecosystems) like Mongolia.

Vegetation data were obtained from the vegetation map in the National Atlas of Mongolia (Institute of Geography, Mongolian Academy of Science, 2009). The vegetation map was first scanned, geometrically corrected, and digitized using the ArcGIS software and then rasterized at 8 km, as was done for the NDVI and climatic datasets. Vegetation types in Mongolia were further grouped into forest, meadow steppe, typical steppe, desert steppe, and alpine steppe. Cropland and Gobi Desert vegetation were neglected in the present study because the first accounted for a very small number of pixels in the 8-km GIMMS NDVI data and the second consisted of very sparse vegetation. As was done in a study at the whole China scale (Piao *et al.*, 2003), it is hypothesized here that the five broad vegetation types (without considering subtypes) mentioned earlier are relatively stable and that this study can ignore land conversion between broad vegetation types in 8-km coarse spatial resolution NDVI images over the study period, primarily due to the long prevalence of nomadic herding in Mongolia, the low population density, and the associated minimal human disturbance (Neupert, 1999; Upton, 2010).

2.3. Method

2.3.1. Calibrating MODIS NDVI to GIMMS NDVI

To study long-term vegetation response to climate change, there is a strong need to combine NDVI data from more than one sensor to cover a sufficiently long time period (Steven *et al.*, 2003; Mao *et al.*, 2012). However, due to

differences among satellites, sensor designs, and resolutions, it is necessary to calibrate from one NDVI product to another and to check the consistency between them (Brown *et al.*, 2008). In the present study, numerous linear regression models (for each pixel) (Equation (1)) were developed to calibrate MODIS NDVI to GIMMS NDVI for each month of the growing season during 2000–2010 by regressing GIMMS NDVI as a function of MODIS NDVI for the overlapping period of 2000–2006:

$$G(k, m) = a(k, m)M(k, m) + b(k, m) + \varepsilon(k, m) \quad (1)$$

where $G(k, m)$ and $M(k, m)$ are the GIMMS NDVI and the MODIS NDVI of pixel k in month m , a and b are the regression coefficients (slope and intercept) obtained by fitting time series to the two NDVIs for each month of 2000–2006, and ε is the residual error. By applying the developed models, a new monthly MODIS NDVI dataset from 2000 to 2010 (called the Extended GIMMS NDVI in the following discussion), which has similar characteristics to the GIMMS NDVI, was generated to extend the traditional GIMMS NDVI up to the present. The correlation analysis and difference values between the 2 monthly NDVI for each biome were examined to evaluate whether consistency had been attained.

2.3.2. Vegetation dynamics and its response to climate change

Based on the vegetation map, time series for growing-season mean NDVI [both GIMMS NDVI (1982–2006) and extended GIMMS NDVI (2000–2010)], temperature, and precipitation and also for monthly NDVI, temperature, and precipitation during 1982–2010 were constructed for each biome by averaging all grid pixels belonging to the same biome. Subsequently, a least-squares linear regression model and a piecewise linear regression model were used to detect vegetation and climate variations during 1982–2010.

The least-squares linear regression model (Piao *et al.*, 2011; Chen *et al.*, 2014) was used to detect gradual trends in the NDVI time series and in climatic variables during the 29-year period (Equation (2)):

$$y = a + bt + \varepsilon \quad (2)$$

where y represents the NDVI time series, t is the year, a is the intercept, b is the linear trend (slope), and ε is the residual of the fit.

Generally, trends in long-term NDVI and climatic data might change or reverse in a particular year (Zhang *et al.*, 2013; Chen *et al.*, 2014). A piecewise linear regression model (Toms and Lesperance, 2003; Tomé and Miranda, 2004) was used to detect the timing and magnitude of potential trend changes in NDVI and climatic variables (Equation (3)):

$$y = \begin{cases} a_0 + b_1t + \varepsilon & t \leq \alpha \\ a_0 + b_1t + b_2(t - \alpha) + \varepsilon & t > \alpha \end{cases} \quad (3)$$

where y is the NDVI or climatic variable time series, t is the year, α is the estimated TP of the time-series trend;

a_0 , b_1 , and b_2 are the regression coefficients; a_0 is the intercept, b_1 and $b_1 + b_2$ are the trends before and after the TP, and ε is the residual error. In the present study, the condition $\alpha \in \{4, 6, \dots, N-4\}$ was imposed to eliminate two consecutive segments before and after the TP with too few data points, as done in a previous study (Chen *et al.*, 2014). The TP was estimated by the maximum likelihood method.

The two models described above were implemented for the NDVI and climatic variables over the growing-season and monthly timescales for each biome. To examine the climatic factors driving the changes in NDVI trends, the Pearson correlation coefficients and p -values (significance level) between NDVI and climatic variables were calculated for each biome. In view of the lagged response of NDVI to climatic variables, the correlations between monthly NDVI and temperature and precipitation for all previous growing-season months in a calendar year were also calculated.

3. Results and discussion

3.1. Calibration from MODIS NDVI to GIMMS NDVI

The scatter plots between growing-season monthly GIMMS NDVI and Extended GIMMS NDVI by biome are shown in Figure 2(a) [7 months (April–October) \times 7 years (2000–2006) = 49 points for each biome]. The results showed high coefficients of determination between the GIMMS NDVI and the new Extended GIMMS NDVI for all biomes, with values around 0.98 except for desert steppe (0.86), a result comparable to those from previous studies (Brown *et al.*, 2008; Mao *et al.*, 2012). The relatively lower R -value for desert steppe was mostly attributable to lower intra-annual NDVI variation in this environment (Fensholt and Proud, 2012). The standard deviation of multi-year average monthly NDVI was lowest for desert steppe (0.009) (Table 1). Another reason for this lower R -value may be the difference between reflectance in the red and near-infrared bands in sparsely vegetated regions like desert steppe when calculating the MODIS NDVI and the GIMMS NDVI (Steven *et al.*, 2003; Fensholt *et al.*, 2009). It is well known that the soil background has a large impact on the reflected signal from a sparsely vegetated region (Fensholt *et al.*, 2009), and the large reflectance difference between the red and near-infrared bands therefore stands out at lower canopy cover (Huete, 1988). The difference values between the two NDVI datasets were mostly concentrated between -0.03 and 0.03 (Figure 2(b)), indicating high consistency and continuity between the two datasets. The high degree of continuity and consistency between the two NDVI datasets can also be clearly observed in Figure 3.

3.2. Interannual variations in growing-season mean NDVI and climatic variables

Figure 3 and Table 2 show the interannual variation of growing-season mean NDVI, temperature, and total

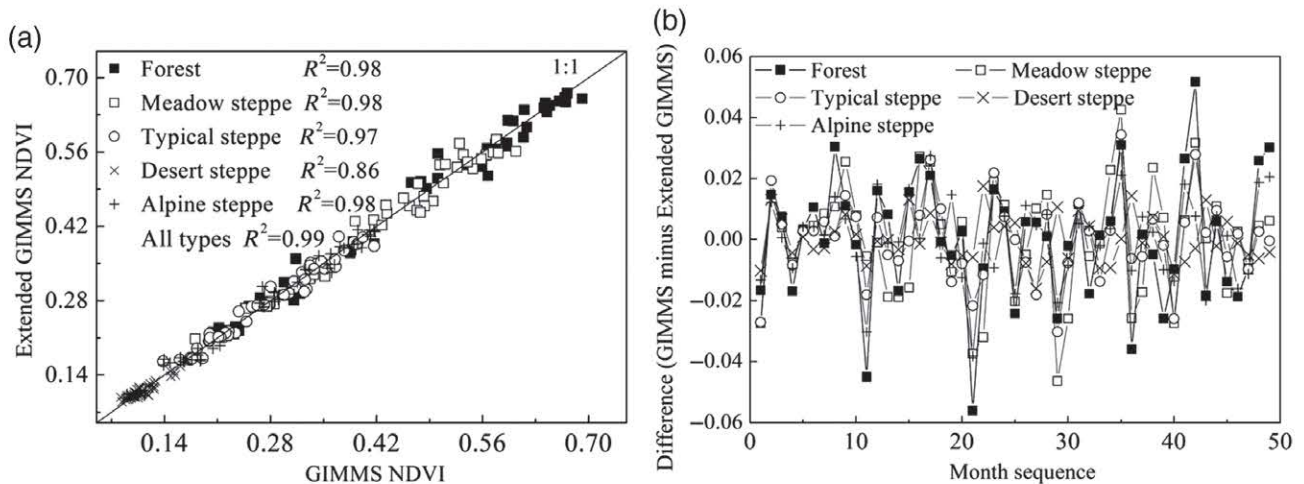


Figure 2. Calibration result from MODIS NDVI to GIMMS NDVI.

Table 1. Standard deviation of multi-year average monthly NDVI by biome.

	Forest	Meadow steppe	Typical steppe	Desert steppe	Alpine steppe
SD	0.161	0.127	0.072	0.009	0.106

precipitation during 1982–2010 in Mongolia for forest, meadow steppe, typical steppe, desert steppe, and alpine steppe. For the entire observation period, the vegetation activity of forest and alpine steppe experienced a significant increasing trend, with annual increments in mean NDVI values of 0.0007 year^{-1} ($p=0.03$) and 0.0009 year^{-1} ($p=0.0003$) (Figure 3(a) and (e)). However, the curves for meadow steppe, typical steppe, and desert steppe vegetation remained nearly flat, and no obvious trend was observed (trend = 0.0001, 0.0001, and $-0.00002 \text{ year}^{-1}$ for meadow steppe, typical steppe, and desert steppe, respectively) over a 29-year period (Figure 3(b)–(d); Table 2). All the piecewise linear models based on 29-year time-series NDVI data predicted a TP year for NDVI trend of 1994 (Figure 3(b)–(e); Table 2), except for forest, where the TP was predicted to occur in 1991 (Figure 3(a)). For the four steppe grassland ecosystems, the NDVI gradually increased until 1994, with the largest increase (0.0025 year^{-1}) occurring in meadow steppe and the lowest (0.0011 year^{-1}) in desert steppe; all these trends then stalled or decreased at a rate of $-0.00002 \text{ year}^{-1}$ (alpine steppe) to $-0.0015 \text{ year}^{-1}$ (meadow steppe). Forest vegetation increased until 1991 at a rate of 0.0025 year^{-1} and showed a flat trend afterward ($0.00006 \text{ year}^{-1}$). This NDVI trend reversal, particularly for meadow steppe, typical steppe, and desert steppe in Mongolia over a 29-year period, is generally consistent with the results of previous studies conducted in the rest of Eurasia and in North America based on shorter data series (1982–2006, 25 years) (Park and Sohn, 2010; Piao *et al.*, 2011; Wang *et al.*, 2011), which demonstrated that the increasing trends in vegetation growth before the late

1990s seem to have stalled or even reversed from that time onward. However, the reversal in Mongolia seems to have occurred about 3–6 years earlier than in the rest of Eurasia and in North America.

Climate records in Mongolia show warming and drying trends for all biomes from 1982 to 2010 (Figure 3), indicating that drought stress and potential desertification stress are major environmental issues in Mongolia. Particularly for forest, meadow steppe, and typical steppe, the increasing temperature trend and the decreasing precipitation trend were both significant at the 1% level (Figure 3(a)–(c)). The piecewise regression model further indicated that pronounced drying trends for most biomes occurred between 1990 and 1994, followed by persistent warming trends until recently. Detailed information including trends, TPs, and intercepts of all modelled vegetation and climate variations can also be clearly seen in Table 2.

3.3. Response of growing-season NDVI to climate change

It can be clearly seen from Table 3 that the relationship between growing-season mean NDVI and climatic variables from the corresponding period strongly varied among biomes, depending mostly on differences in the climate limiting factor for plant growth in the different biomes. For forest, regardless of the observation period, growing-season NDVI was positively correlated with temperature, particularly for the entire observation period ($R=0.47$, $p=0.009$), but negatively with precipitation ($R=-0.34$, $p=0.07$), indicating that against the background of global warming, rising temperatures were beneficial to forest growth in Mongolia during the previous 29-year period. This observation is in agreement with previous studies suggesting that temperature is a decisive climatic factor for vegetation growth in northern high latitudes (Zhou *et al.*, 2001; Ichii *et al.*, 2002; Nemani *et al.*, 2003) and that an increase in temperature could enhance forest growth by lengthening the growing period and enhancing photosynthesis (Zhou *et al.*, 2001; Piao

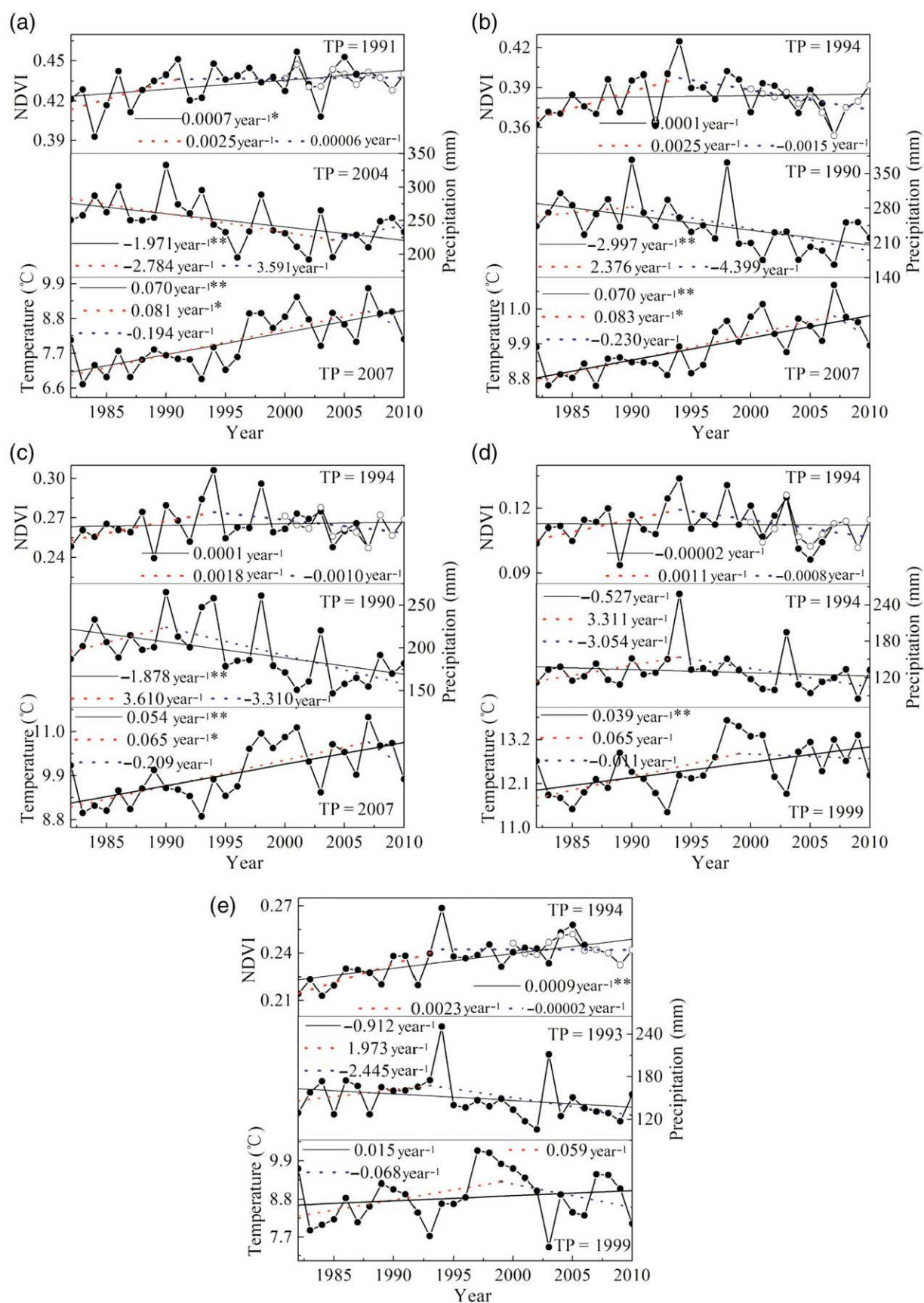


Figure 3. Interannual variations of growing-season mean NDVI, temperature, and precipitation from 1982–2010 for (a) forest, (b) meadow steppe, (c) typical steppe, (d) desert steppe, and (e) alpine steppe. The extended GIMMS NDVI is indicated by the symbol \circ . ** and * indicate $p < 0.01$, $p < 0.05$ respectively.

Table 2. Linear regression models and piecewise linear regression models for 1982–2010 by biome. y_n , y_p , and y_t represent NDVI, precipitation, and temperature, respectively, and t represents the year.

Biome	Linear regression models	Piecewise linear regression models
Forest	$y_n = -0.9309 + 0.0007t$ $y_p = 4183.02 - 1.971t$ $y_t = -131.71 + 0.070t$	$y_n = \begin{cases} -4.578 + 0.0025t & t \leq 1991 \\ -4.578 + 0.0025t - 0.0025(t - 1991) & t > 1991 \end{cases}$ $y_p = \begin{cases} 5802.18 - 2.785t & t \leq 2004 \\ 5802.18 - 2.785t + 6.376(t - 2004) & t > 2004 \end{cases}$ $y_t = \begin{cases} -153.29 + 0.081t & t \leq 2007 \\ -153.29 + 0.081t - 0.275(t - 2007) & t > 2007 \end{cases}$
Meadow steppe	$y_n = 0.163 + 0.0001t$ $y_p = 6231.46 - 2.998t$ $y_t = -130.76 + 0.070t$	$y_n = \begin{cases} -4.683 + 0.0025t & t \leq 1994 \\ -4.683 + 0.0025t - 0.0040(t - 1994) & t > 1994 \end{cases}$ $y_p = \begin{cases} -4446.3 + 2.376t & t \leq 1990 \\ -4446.3 + 2.376t - 6.776(t - 1990) & t > 1990 \end{cases}$ $y_t = \begin{cases} -155.28 + 0.083t & t \leq 2007 \\ -155.28 + 0.083t - 0.313(t - 2007) & t > 2007 \end{cases}$
Typical steppe	$y_n = 0.028 + 0.0001t$ $y_p = 3944.95 - 1.878t$ $y_t = -97.808 + 0.054t$	$y_n = \begin{cases} -3.255 + 0.0018t & t \leq 1994 \\ -3.255 + 0.0018t - 0.0027(t - 1994) & t > 1994 \end{cases}$ $y_p = \begin{cases} -6959.39 + 3.609t & t \leq 1990 \\ -6959.39 + 3.609t - 6.919(t - 1990) & t > 1990 \end{cases}$ $y_t = \begin{cases} -119.26 + 0.065t & t \leq 2007 \\ -119.26 + 0.065t - 0.273(t - 2007) & t > 2007 \end{cases}$
Desert steppe	$y_n = 0.157 - 0.00002t$ $y_p = 1181.95 - 0.527t$ $y_t = -64.569 + 0.039t$	$y_t = \begin{cases} -2.171 + 0.0011t & t \leq 1994 \\ -2.171 + 0.0011t - 0.0019(t - 1994) & t > 1994 \end{cases}$ $y_p = \begin{cases} -6449.14 + 3.311t & t \leq 1994 \\ -6449.14 + 3.311t - 6.356(t - 1994) & t > 1994 \end{cases}$ $y_t = \begin{cases} -117.40 + 0.065t & t \leq 1999 \\ -117.40 + 0.065t - 0.077(t - 1999) & t > 1999 \end{cases}$
Alpine steppe	$y_n = -1.575 + 0.0009t$ $y_p = 1971.6 - 0.913t$ $y_t = -21.107 + 0.015t$	$y_n = \begin{cases} -4.383 + 0.0023t & t \leq 1994 \\ -4.383 + 0.0023t - 0.0023(t - 1994) & t > 1994 \end{cases}$ $y_p = \begin{cases} -3764.4 + 1.973t & t \leq 1993 \\ -3764.4 + 1.973t - 4.417(t - 1993) & t > 1993 \end{cases}$ $y_t = \begin{cases} -108.42 + 0.059t & t \leq 1999 \\ -108.42 + 0.059t - 0.127(t - 1999) & t > 1999 \end{cases}$

Table 3. Correlations between growing-season NDVI and climate variables for different biomes: growing-season precipitation (P), growing-season temperature (T); ESP, BTP, ATP represent the entire study period, before the turning point, and after the turning point.

Biome	Precipitation			Temperature		
	ESP	BTP	ATP	ESP	BTP	ATP
Forest	-0.34*	0.26	-0.41*	0.47***	0.36	0.32
Meadow steppe	0.35*	0.35	0.52**	-0.11	0.30	-0.51**
Typical steppe	0.62***	0.73***	0.85***	-0.08	-0.14	-0.19
Desert steppe	0.74***	0.78***	0.79***	-0.17	-0.32	-0.20
Alpine steppe	0.15	0.77***	0.43*	0.13	-0.02	-0.15

***, **, and * indicate $p < 0.01$, $p < 0.05$, and $p < 0.1$, respectively.

et al., 2011). However, excessive precipitation may restrict forest growth due to precipitation-accompanied reductions in solar radiation and temperature (Mao *et al.*, 2012).

In contrast, there were significant positive correlations between NDVI and precipitation for meadow steppe ($R = 0.35$, $p = 0.06$), typical steppe ($R = 0.62$, $p = 0.0004$), and desert steppe ($R = 0.74$, $p < 0.0000$), but negative correlations between NDVI and temperature ($R = -0.11$,

$p = 0.57$; $R = -0.08$, $p = 0.67$; $R = -0.17$, $p = 0.39$) for the same biomes from 1982 to 2010 (Table 3). Moreover, the patterns of NDVI fluctuation, particularly for typical steppe (Figure 3(c)) and desert steppe (Figure 3(d)), corresponded closely to that of precipitation. Peak NDVI values observed in 1990, 1994, 1998, and 2003 corresponded closely to peak precipitation in the same year, and lower NDVI values in 1982, 1992, 1995, 1999, 2004, and 2007

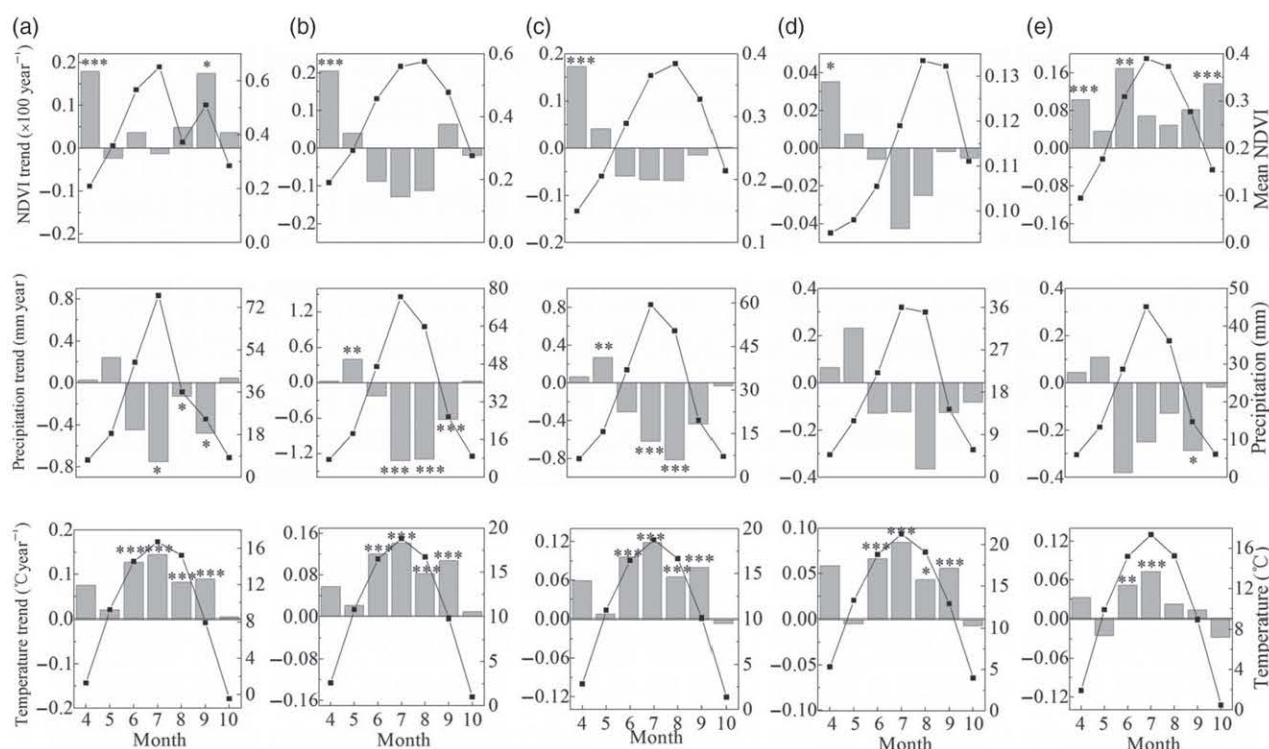


Figure 4. Dynamics of monthly NDVI and climatic variables from 1982 to 2010 for five biome types: (a) forest, (b) meadow steppe, (c) typical steppe, (d) desert steppe, and (e) alpine steppe. The bars represent trends, and the lines denote mean values. ***, **, and * indicate $p < 0.01$, $p < 0.05$, and $p < 0.1$, respectively.

corresponded well with lower precipitation, implying that rainfall is a direct factor regulating vegetation variation in grasslands, an observation which is in agreement with previous findings (Hoffmann and Jackson, 2000; Piao *et al.*, 2006b). In addition, positive correlations with precipitation increased obviously from meadow steppe to typical steppe and then to desert steppe, implying that the sensitivity of vegetation to precipitation may increase in extremely arid regions as aridity increases. However, against the background of global warming, the heat conditions are sufficient for grass growth in steppe-dominated regions in Mongolia, and rising temperatures could increase drought stress and thereby restrict grass growth (negative correlation). For alpine steppe, the effects of precipitation on vegetation dynamics seem to be stronger than those of temperature on both sides of the TP but are not obvious over the entire study period (Table 3).

Generally, the TPs of the growing-season mean NDVI trends were not always coupled with those of climatic variables (Figure 3, Table 2). For forest, the TPs of climatic variables, both temperature and precipitation, arrived later than that of NDVI. However, for steppe grassland ecosystems, the TP of precipitation occurred earlier than that of NDVI, whereas the TP of temperature arrived later than that of NDVI. These findings suggested that perhaps the TP of NDVI as detected by the piecewise linear regression model may be very complex and attributable to the combined influence of numerous variables, not only temperature and precipitation but also other climatic and non-climatic factors.

3.4. Response of monthly NDVI to climate change

3.4.1. Dynamics of monthly NDVI and climatic variables

Variations in growing-season NDVI can be attributed mostly to trends in monthly NDVI (Piao *et al.*, 2003), and monthly scale analysis can detect more detailed NDVI change signals and their contribution to growing-season NDVI trend (Chen *et al.*, 2014). Figure 4 shows the mean values and change trends of monthly NDVI over 1982–2010 by biome in Mongolia. For forest, the NDVI trends for all months increased except for May and July, with the largest increases occurring in April (trend: 0.0018 year^{-1} , $R = 0.60$, $p = 0.0007$) and September (trend: 0.0017 year^{-1} , $R = 0.34$, $p = 0.07$) (Figure 4(a), top), implying that the forest ecosystem in Mongolia tends to exhibit an earlier start of the growing season and delayed dormancy (i.e. lengthening of the growing season) (Zhou *et al.*, 2001; Park and Sohn, 2010; Piao *et al.*, 2011). This observation is also in agreement with others made in forest in China by Piao *et al.* (2003), who found that the largest increases in forest NDVI in China took place mostly in April, May, and September. By comparison, NDVI values for meadow steppe, typical steppe, and desert steppe significantly increased in April by 0.0021 year^{-1} ($R = 0.75$, $p < 0.0000$), 0.0017 year^{-1} ($R = 0.78$, $p < 0.0000$), and 0.0004 year^{-1} ($R = 0.36$, $p = 0.05$), respectively, and decreased in almost all summer and autumn months (Figure 4(b)–(d), top). However, the NDVI values for all growing-season months increased

Table 4. TPs of monthly NDVI, temperature, and precipitation during 1982–2010.

	April	May	June	July	August	September	October
Forest							
NDVI	1985	1990	1985	1985	1988	1985	1995
Precipitation	1985	2003	2005	1993	2006	1991	1996
Temperature	2007	2006	2002	2002	2007	1992	1985
Meadow steppe							
NDVI	1989	2001	1985	1988	1990	1996	1998
Precipitation	2004	2007	2005	1990	2006	1990	1987
Temperature	2007	2006	1989	2002	2007	1992	2000
Typical steppe							
NDVI	1989	2002	1988	1990	1994	1996	1998
Precipitation	1985	1988	2005	1993	1990	1991	2005
Temperature	2007	2000	2001	2000	2007	1992	1985
Desert steppe							
NDVI	1989	2001	2000	1994	1994	1994	1998
Precipitation	2007	2003	1994	1994	1994	2007	2005
Temperature	2007	2000	2001	2000	2001	1985	1986
Alpine steppe							
NDVI	1988	1997	2002	1986	1985	1995	2006
Precipitation	2007	2003	2007	1993	1991	2006	2004
Temperature	2007	1999	2000	1999	2000	1992	1985

significantly for alpine steppe, with the largest annual increase of 0.0017 year^{-1} ($R = 0.42$, $p = 0.02$) occurring in June and the lowest occurring in May (Figure 4(e), top). The trends in monthly climatic variables for all biome types, on the whole, showed warming and weak wetting trends at the beginning of the growing season, followed by significant warming and drying trends in the middle and at the end of the growing season, particularly for meadow steppe and typical steppe (Figure 4(b) and (c), middle and bottom), over the entire observation period. Intra-annual variations of NDVI and climatic variables for all biomes showed a similar pattern, with maximum values occurring in July or August.

Table 4 and Figure 5 show the TPs of monthly NDVI and climatic variables and their trends on both sides of the TPs. The detected TPs of monthly NDVI were not exactly coupled with climatic variables and varied strongly by month and by biome, with the earliest TP occurring in 1985 and the latest occurring in 2006. In comparison, the TPs of monthly NDVI for forest seem to have arrived earlier than for steppe grassland ecosystems generally.

From Figure 5, it can be clearly seen that opposite trends occurred on both sides of the TPs of all monthly NDVIs for all biomes. The monthly NDVIs for all biomes increased until the TP from May to October at a rate of 0.0003 year^{-1} (May, desert steppe) (Figure 5(d), top) to 0.0349 year^{-1} (June, meadow steppe) (Figure 5(b), top) and stalled or even decreased afterward at a rate of $-0.0055 \text{ year}^{-1}$ (May, meadow steppe) (Figure 5(b), top) to $-0.00001 \text{ year}^{-1}$ (September, alpine steppe) (Figure 5(e), top). An opposite phenomenon occurred in April, with a decreasing trend before the TP [$-0.0014 \text{ year}^{-1}$ for desert steppe (Figure 5(d), top) to $-0.0111 \text{ year}^{-1}$ for forest (Figure 5(a), top)] and a pronounced increasing trend after the TP [0.0007 year^{-1} for desert steppe (Figure 5(d), top) to 0.0028 year^{-1}

for meadow steppe (Figure 5(b), top)], suggesting that widespread vegetation greening (i.e. increasing NDVI) appears to dominate at the beginning of the growing season (April) after the TP. For forest, vegetation greening at the end of the growing season (September) was also very significant after the TP (Figure 5(a), top). At a monthly scale, the drying and warming climate appeared to dominate in summer months after the TP for most biomes.

3.4.2. Same-time response of monthly NDVI to climate change

To examine climate impacts on vegetation dynamics at a finer temporal scale, correlations between monthly NDVI and climatic variables were calculated during 1982–2010 (Table 5). For forest, the NDVI was correlated positively and significantly with temperature over all growing-season months except July, particularly for April ($R = 0.53$, $p = 0.003$), May ($R = 0.68$, $p < 0.0000$), June ($R = 0.48$, $p = 0.008$), and October ($R = 0.50$, $p = 0.005$). These results further confirmed the finding from previous studies that the large increase in NDVI over northern mid-to high latitudes can mainly be attributed to warming temperatures at the beginning and end of the growing season (Myneni *et al.*, 1997; Zhou *et al.*, 2001; Nemani *et al.*, 2003). However, it should also be noted that increasing temperature in the middle of the growing season (except for July) also plays a significant role in forest enhancement in Mongolia. An opposite relationship was found between forest NDVI and precipitation for all months except June ($R = 0.19$, $p = 0.34$), particularly in August ($R = -0.33$, $p = 0.08$), September ($R = -0.35$, $p = 0.06$), and October ($R = -0.38$, $p = 0.04$). This implies that perhaps precipitation in previous months, including snowfall during the winter, is preserved better in the soil of forest-dominated areas in Mongolia than elsewhere and that excessive

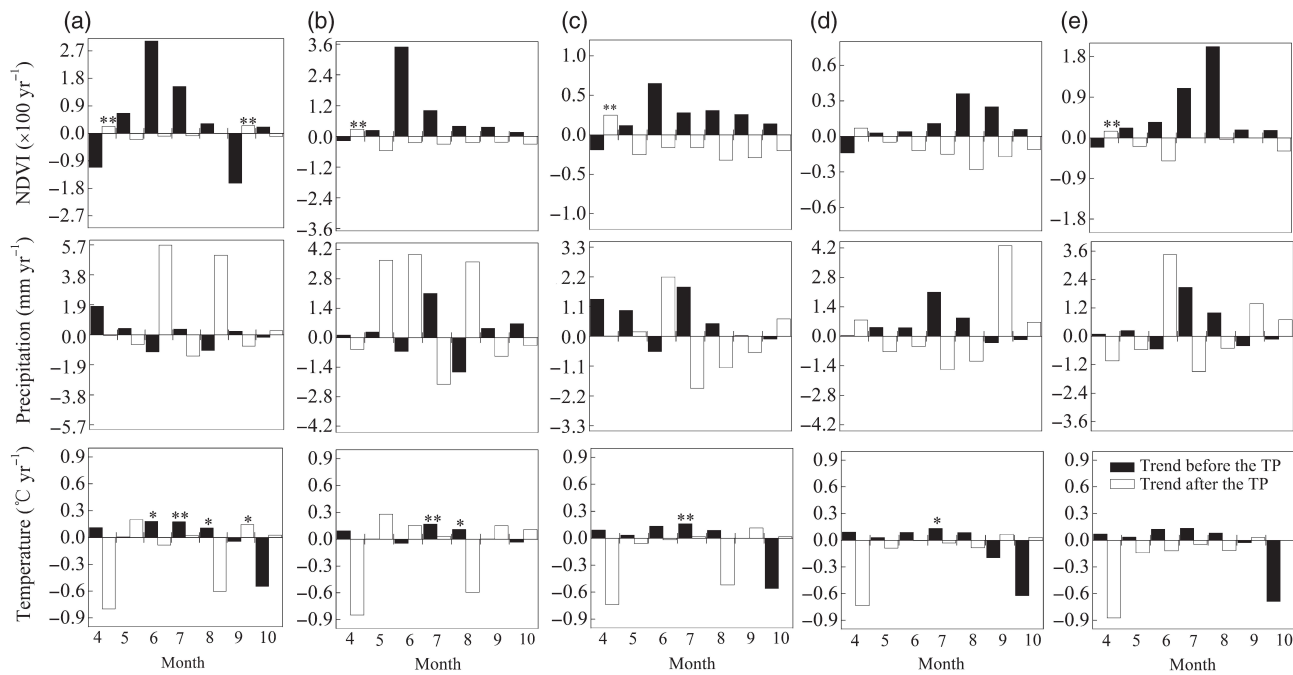


Figure 5. Dynamics of monthly NDVI and climatic variables from 1982 to 2010 for five biome types: (a) forest, (b) meadow steppe, (c) typical steppe, (d) desert steppe, and (e) alpine steppe.

Table 5. Correlation between monthly NDVI and corresponding climate variables for different biomes: monthly precipitation (P), monthly temperature (T).

Biome type	Climate variable	Correlation coefficient						
		April	May	June	July	August	September	October
Forest	P	-0.27	-0.03	0.19	-0.21	-0.33*	-0.35*	-0.38**
	T	0.53***	0.68***	0.48***	-0.04	0.32*	0.30	0.50***
Meadow steppe	P	0.04	0.16	0.22	0.43**	0.08	0.004	0.04
	T	0.24	0.38**	0.07	-0.37**	-0.31	0.13	0.25
Typical steppe	P	0.19	0.38**	0.43**	0.47***	0.39**	-0.03	0.05
	T	0.18	0.20	0.08	-0.44**	-0.43**	0.21	0.21
Desert steppe	P	-0.03	0.20	0.17	0.58***	0.52***	0.13	0.20
	T	-0.23	-0.07	0.07	-0.32*	-0.30	0.21	-0.21
Alpine steppe	P	-0.02	-0.41**	0.02	0.16	0.27	-0.24	-0.20
	T	0.37**	0.65***	0.67***	0.01	-0.13	0.28	0.31

***, **, and * indicate $p < 0.01$, $p < 0.05$, and $p < 0.1$, respectively.

rainfall could depress forest growth in the same month by reducing temperature and radiation, particularly in autumn months (Mao *et al.*, 2012). This can be further confirmed by the lagged time responses to climate change (Section 3.4.3). Alternatively, this effect might also arise from seasonally frozen ground in forest regions, which could provide adequate moisture during the growing season (Han *et al.*, 2014). Unlike that in forest ecosystems, NDVI for almost all growing-season months was, in general, positively correlated with precipitation for meadow steppe, typical steppe, and desert steppe and was related positively to temperature in the early and late growing season, but negatively and significantly in July (meadow: $R = -0.37$, $p = 0.05$; typical: $R = -0.44$, $p = 0.02$; desert: $R = -0.32$, $p = 0.10$) and August (meadow: $R = -0.31$, $p = 0.10$; typical: $R = -0.43$, $p = 0.02$; desert: $R = -0.30$, $p = 0.10$). However, the strength of the correlation differed markedly

among the different kinds of steppe. For example, the NDVI of meadow steppe was more closely related with temperature in May ($R = 0.38$, $p = 0.04$) than that of typical steppe ($R = 0.20$, $p = 0.30$) and desert steppe ($R = -0.07$, $p = 0.72$). In contrast, the NDVIs of typical steppe and desert steppe were more strongly correlated with precipitation than that of meadow steppe, particularly in July and August. There was also an opposite correlation between NDVI and temperature in April, May, and October for typical steppe ($R = 0.18$, $p = 0.36$; $R = 0.20$, $p = 0.30$; $R = 0.21$, $p = 0.26$) and desert steppe ($R = -0.23$, $p = 0.24$; $R = -0.07$, $p = 0.72$; $R = -0.21$, $p = 0.27$).

These discrepancies in the response to monthly climate variables among the various kinds of steppe could be associated with their different climatic growth environments, as represented by factors such as moisture index and thermal condition. Figure 6 shows the variation of

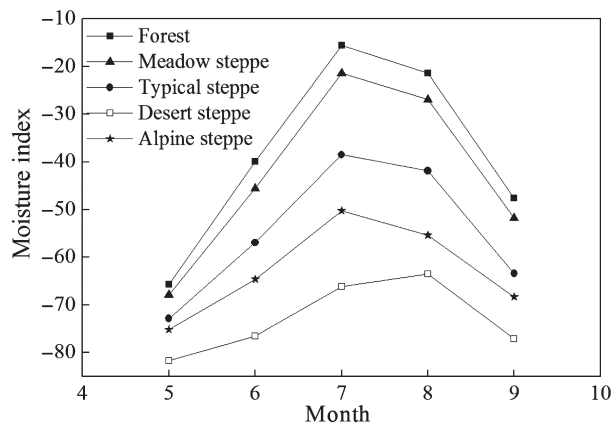


Figure 6. Variation of multi-year mean monthly moisture index by biome.

Thornthwaite's moisture index (Thornthwaite, 1948) for different biome types. From meadow steppe to typical steppe and then to desert steppe, the moisture index decreased for all growing-season months, with the largest differences in July and August (Figure 6). Therefore, the relationship between monthly NDVI and precipitation became stronger as the moisture index decreased from meadow steppe to typical steppe and then to desert steppe, particularly in July and August, because the largest difference in moisture index occurred in July and August. In contrast, meadow steppe in Mongolia is generally distributed under conditions with more moisture and lower temperature than those of typical and desert steppe, and therefore there was a stronger positive correlation with temperature in May than for typical and desert steppe. However, the negative impact of temperature on meadow steppe vegetation growth in July and August was still more significant in Mongolia (Table 5), implying that vegetation growth of meadow steppe in Mongolia is strongly hindered by rising temperature-induced drought conditions in mid- and late summer. This phenomenon is inconsistent with that observed in temperate meadow in China by Piao, who suggested a positive correlation between meadow NDVI and temperature in summer (Piao *et al.*, 2006b). For alpine steppe, the monthly NDVI was significantly and positively related to temperature in April ($R = 0.37$, $p = 0.05$), May ($R = 0.65$, $p = 0.0001$), and June ($R = 0.67$, $p < 0.0000$), but negatively to precipitation in May ($R = -0.41$, $p = 0.03$) (Table 5), indicating that temperature in the early growing season and in early summer (June) has a strong positive influence on alpine steppe vegetation growth in Mongolia. The negative correlation with precipitation was not consistent with the results for alpine meadow on the Tibetan Plateau reported by Piao, where positive correlations were observed (Piao *et al.*, 2006a).

3.4.3. Lagged time response of monthly NDVI to climate change

Even as climate factors change, vegetation growth takes time to respond, and time lags most likely vary for different

climate factors and different areas (Braswell *et al.*, 1997; Hu *et al.*, 2011) because of delays in the adjustment of soil moisture content and biological processes (Davenport and Nicholson, 1993). Figure 7 shows the correlation coefficients between monthly NDVI and climatic variables in all previous months for each biome type during 1982–2010. The lag period and the strength of the lag effect of climate varied by biome and by month. For forest, significant positive correlations were found between NDVI in April ($R = 0.33$, $p = 0.08$), May ($R = 0.33$, $p = 0.08$), and September ($R = 0.44$, $p = 0.02$) and temperature from the preceding month (Figure 7(a)), implying that there exists a 1-month lag effect of temperature on forest NDVI in the early growing season and in late summer (August). However, the strength of this relationship was much less than that of the relationship with no time lag (Table 5), suggesting that temperature conditions in the same month may be more critically important to forest growth at the beginning and end of the growing season in Mongolia. Unlike the negative effect of precipitation on NDVI in the same month, there was always a positive precipitation lag effect on forest NDVI except in May, September, and October (Figure 7(b)). This may have been the reason for a significant negative correlation between NDVI and precipitation in the same month (Table 5), because precipitation from the preceding month could maintain enough moisture in the deeper-rooted forest system, in which case precipitation in the same month may lead to surplus water, thereby depressing forest growth.

Similarly to forest, almost all NDVI values for meadow steppe, typical steppe, and desert steppe in April, May, and October were positively but weakly correlated with temperature in the preceding month (Figure 7(c), (e), and (g)), indicating that higher temperatures in the preceding month could favour grass growth at the beginning and end of the growing season. However, temperatures in May, June, July, and August had about a 1- to 3-month lagged negative effect on grass growth. A similar trend was observed in the whole of China by Piao, who demonstrated an approximately 3-month lag effect of temperature on vegetation (Piao *et al.*, 2003). However, the positive lagged effect of precipitation on the three steppe types was more significant, and the period of the lag varied by month (Figure 7(d), (f), and (h)). Generally, there is a 1-month lag effect on vegetation response to precipitation in March, April, and May and a 1- to 4-month lag effect from precipitation in June, July, and August, suggesting that spring and summer precipitation is a key factor for annual vegetation growth in Mongolia, particularly for grass growth in the middle and at the end of the growing season. This long-term effect of precipitation in summer on grass growth in Mongolia is longer than that observed by Shinoda in dry savannas in Africa, where there existed at most a 2.5-month lag effect (Shinoda, 1995). In addition, almost all the lag effects of precipitation are stronger than that with no time lag (Table 5), suggesting the importance of antecedent precipitation conditions for grass growth. For alpine grassland, temperature

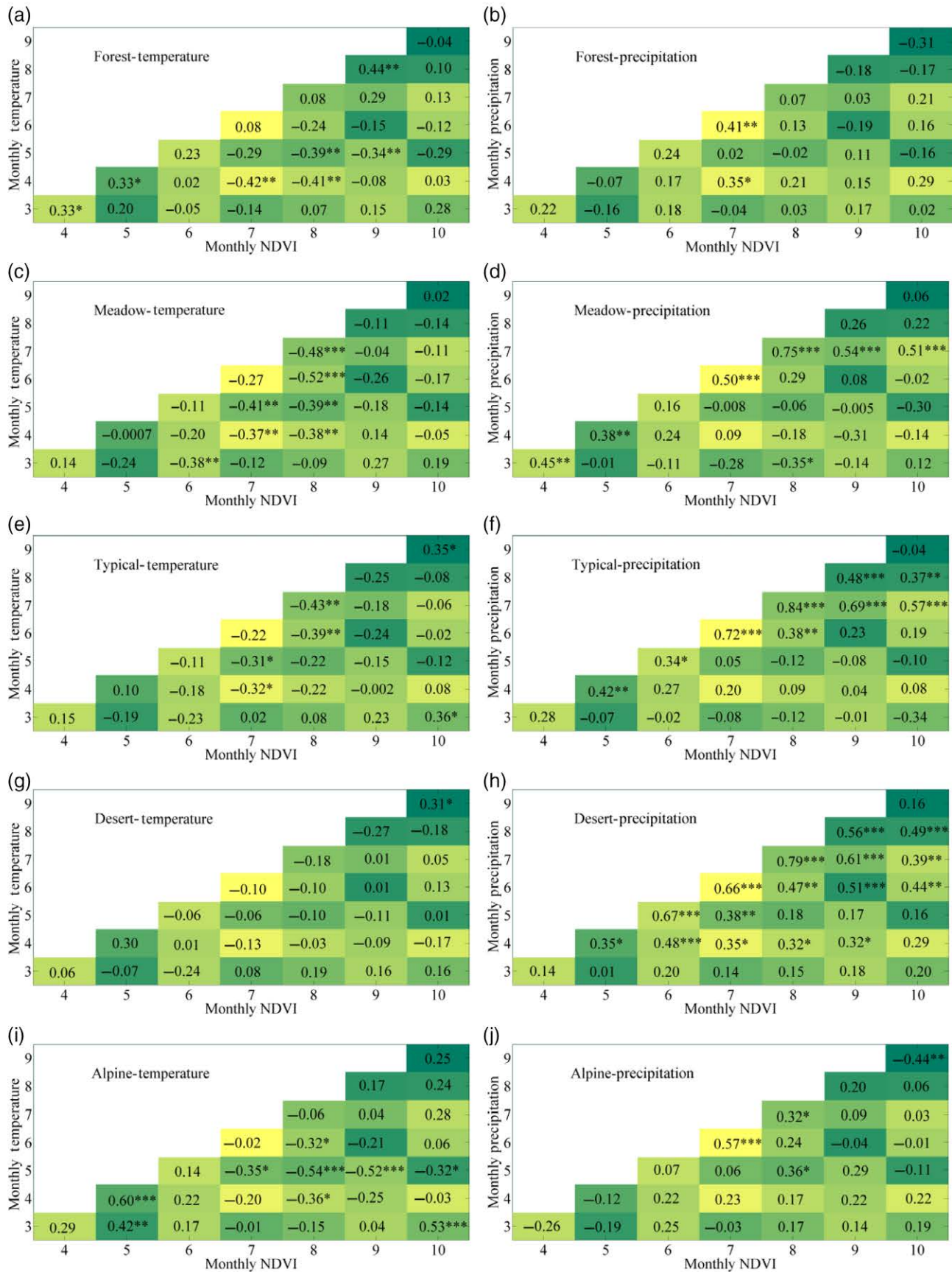


Figure 7. Correlation between monthly NDVI and climatic variables from all previous months by biome during 1982–2010. ***, **, and * indicate $p < 0.01$, $p < 0.05$, and $p < 0.1$, respectively.

for March, April, May, August, and September shows a positive relationship with NDVI in the subsequent 1 or 2 months (Figure 7(i)), indicating that rising temperature during these months is favourable for alpine grass growth, particularly temperature in March and April, whereas an opposite trend was observed in the correlations between NDVI in July and August and the two climatic variables from preceding months.

4. Conclusions

In this study, a monthly NDVI sequence has been developed for Mongolia covering the period 1982–2010 by calibrating the MODIS NDVI (2000–2010) to the GIMMS NDVI (1982–2006) based on the overlapping period of 2000–2006. The calibration results from pixel-based models demonstrated that the continuity and consistency of the newly constructed NDVI are in acceptable agreement with the GIMMS NDVI for each biome and can detect subtle trends in the long-term vegetation dynamics of Mongolia. Based on these NDVI datasets and climatic variables (temperature and precipitation) from 1982 to 2010, the growing-season and monthly vegetation dynamics for five biomes and their response to regional climate change have been thoroughly investigated. The results show that vegetation growth for all biomes in Mongolia reversed (from an increasing to a decreasing trend) between 1991 and 1994 and that desertification is becoming one of the most significant ecological stresses in Mongolia for most biomes, particularly for meadow steppe, typical steppe, and desert steppe. This TP of vegetation growth trend in Mongolia was about 3–6 years earlier than in the rest of Eurasia. Pronounced drying trends occurring between 1990 and 1994 and a persistently warming climate until recently have likely played a major role in the NDVI trend reversal. However, the timing of the NDVI trend reversal (TP year) at both growing-seasonal scale and monthly scale was not exactly coupled with the TP of either precipitation or temperature, implying a nonlinear response of trend reversal in vegetation growth to any single climatic variable. On a long-term scale, the impacts of climate change on vegetation growth varied greatly among different biomes, months, and climates due to differences in growth environments and their corresponding climatic regimes. Generally, growing-season NDVI was positively related to temperature and negatively to precipitation for forest, and opposite trends in the correlations between NDVI and temperature and NDVI and precipitation were observed in steppe grassland ecosystems. In addition, this study also shows that the long-time lag effects of climatic variables on vegetation growth are different in different biomes, mostly varying from 1- to 4-month lags, and also vary by climatic variable and by month. This study will be significant for improving our understanding of ecological evolution and highlighting early signs for prevention of natural hazards like desertification and sandstorms in Mongolia and other surrounding East Asian regions such as North China and Korea.

Acknowledgements

This study was supported by the National Natural Science Foundation of China (grant no: 41301456), the national 'twelve-five' Technology Support Project of China (grant no: 2013BAK05B01), the National Basic Research Program of China (973 Program) (grant no: 2010CB951504), and the International Science and Technology Cooperation Project of China (2012DFA31290). We would like to thank the anonymous reviewers for providing constructive suggestions and also to thank the MODIS and AVHRR science teams for providing accessible data products.

References

- Braswell B, Schimel D, Linder E, Moore B. 1997. The response of global terrestrial ecosystems to interannual temperature variability. *Science* **278**(5339): 870–873, doi: 10.1126/science.278.5339.870.
- Brown ME, Lary DJ, Vrieling A, Stathakis D, Mussa H. 2008. Neural networks as a tool for constructing continuous NDVI time series from AVHRR and MODIS. *Int. J. Remote Sens.* **29**(24): 7141–7158, doi: 10.1080/01431160802238435.
- Chen B, Xu G, Coops NC, Ciais P, Innes JL, Wang G, Myneni RB, Wang T, Krzyzanowski J, Li Q. 2014. Changes in vegetation photosynthetic activity trends across the Asia-Pacific region over the last three decades. *Remote Sens. Environ.* **144**: 28–41, doi: 10.1016/j.rse.2013.12.018.
- Chuai XW, Huang XJ, Wang WJ, Bao G. 2013. NDVI, temperature, and precipitation changes and their relationships with different vegetation types during 1998–2007 in Inner Mongolia, China. *Int. J. Climatol.* **33**(7): 1696–1706, doi: 10.1002/joc.3543.
- Davenport M, Nicholson S. 1993. On the relation between rainfall and the normalized difference vegetation index for diverse vegetation types in East Africa. *Int. J. Remote Sens.* **14**(12): 2369–2389, doi: 10.1080/01431169308954042.
- Eastman JR, Sangermano F, Machado EA, Rogan J, Anyamba A. 2013. Global trends in seasonality of normalized difference vegetation index (NDVI), 1982–2011. *Remote Sens.* **5**(10): 4799–4818, doi: 10.3390/rs5104799.
- Eckert S, Hüsler F, Liniger H, Hodel E. 2015. Trend analysis of MODIS NDVI time series for detecting land degradation and regeneration in Mongolia. *J. Arid Environ.* **113**: 16–28.
- Fensholt R, Proud SR. 2012. Evaluation of Earth observation-based global long-term vegetation trends – comparing GIMMS and MODIS global NDVI time series. *Remote Sens. Environ.* **119**: 131–147, doi: 10.1016/j.rse.2009.04.004.
- Fensholt R, Rasmussen K, Nielsen TT, Mbow C. 2009. Evaluation of Earth observation-based long-term vegetation trends – intercomparing NDVI time series trend analysis consistency of Sahel from AVHRR GIMMS, Terra MODIS, and SPOT VGT data. *Remote Sens. Environ.* **113**: 1886–1898, doi: 10.1016/j.rse.2009.04.004.
- Fernandez-Gimenez M, Allen-Diaz B. 2001. Vegetation change along gradients from water sources in three grazed Mongolian ecosystems. *Plant Ecol.* **157**(1): 101–118, doi: 10.1023/A:1014519206041.
- Fujiwara H, Fukuyama T, Shirato Y, Ohkuro T, Taniyama I, Zhang TH. 2007. Deposition of atmospheric ¹³⁷Cs in Japan associated with the Asian dust event of March 2002. *Sci. Total Environ.* **384**(1–3): 306–315, doi: 10.1016/j.scitotenv.2007.05.024.
- Han L, Tsunekawa A, Tsubo M, He C, Shen M. 2014. Spatial variations in snow cover and seasonally frozen ground over northern China and Mongolia, 1988–2010. *Glob. Planet. Change* **116**: 139–148, doi: 10.1016/j.gloplacha.2014.02.008.
- Hoffmann WA, Jackson RB. 2000. Vegetation-climate feedbacks in the conversion of tropical savanna to grassland. *J. Clim.* **13**(9): 1593–1602, doi: 10.1175/1520-0442(2000)013<1593:VCFITC>2.0.CO;2.
- Holben BN. 1986. Characteristics of maximum-value composite images from temporal AVHRR data. *Int. J. Remote Sens.* **7**(11): 1417–1434, doi: 10.1080/01431168608948945.
- Hu MQ, Mao F, Sun H, Hou YY. 2011. Study of normalized difference vegetation index variation and its correlation with climate factors in the three-river source region. *Int. J. Appl. Earth Obs. Geoinf.* **13**(1): 24–33, doi: 10.1016/j.jag.2010.06.003.

- Huete AR. 1988. A soil-adjusted vegetation index (SAVI). *Remote Sens. Environ.* **25**(3): 295–309, doi: 10.1016/0034-4257(88)90106-X.
- Huete AR, Didan K, Miura T, Rodriguez EP, Gap X, Ferreira LG. 2002. Overview of the radiometric and biophysical performance of the MODIS vegetation indices. *Remote Sens. Environ.* **83**: 195–213.
- Huntley BJ, Webb T. 1988. *Vegetation History*. Kluwer: Dordrecht, The Netherlands.
- Ichii K, Kawabata A, Yamaguchi Y. 2002. Global correlation analysis for NDVI and climatic variables and NDVI trends: 1982–1990. *Int. J. Remote Sens.* **23**(18): 3873–3878, doi: 10.1080/01431160110119416.
- Jiang DJ, Fu XF, Wang K. 2013. Vegetation dynamics and their response to freshwater inflow and climate variables in the Yellow River Delta, China. *Quat. Int.* **304**: 75–84, doi: 10.1016/j.quaint.2012.10.059.
- Li X, Cheng GD, Lu L. 2005. Spatial analysis of air temperature in the Qinghai-Tibet Plateau. *Arct. Antarct. Alp. Res.* **37**(2): 246–252.
- Li SG, Eugster W, Asanuma J, Kotani A, Davaa G, Oyunbaatar D, Sugita M. 2008. Response of gross ecosystem productivity, light use efficiency, and water use efficiency of Mongolian steppe to seasonal variations in soil moisture. *J. Geophys. Res.* **113**(G1): G01019, doi: 10.1029/2006JG000349.
- Lu Y, Zhuang Q, Zhou G, Sirin A, Melillo J, Kicklighter D. 2009. Possible decline of the carbon sink in the Mongolian Plateau during the 21st century. *Environ. Res. Lett.* **4**(4): 045023, doi: 10.1088/1748-9326/4/4/045023.
- Mao DH, Wang ZM, Luo L, Ren CY. 2012. Integrating AVHRR and MODIS data to monitor NDVI changes and their relationships with climatic parameters in Northeast China. *Int. J. Appl. Earth Obs. Geoinf.* **18**: 528–536, doi: 10.1007/s11442-013-1062-2.
- Myneni RB, Keeling C, Tucker C, Asrar G, Nemani RR. 1997. Increased plant growth in the northern high latitudes from 1981 to 1991. *Nature* **386**(6626): 698–702, doi: 10.1038/386698a0.
- National Statistical Office of Mongolia. 2011. *Mongolian Statistical Yearbook*. National Statistical Office of Mongolia: Ulaanbaatar, 19–20.
- Nemani RR, Keeling CD, Hashimoto H, Jolly WM, Piper SC, Tucker CJ, Myneni RB, Running SW. 2003. Climate-driven increases in global terrestrial net primary production from 1982 to 1999. *Science* **300**(5625): 1560–1563, doi: 10.1126/science.1082750.
- Neupert RF. 1999. Population, nomadic pastoralism, and the environment in the Mongolian Plateau. *Popul. Environ.* **20**(5): 413–441.
- Park HS, Sohn B. 2010. Recent trends in changes of vegetation over East Asia coupled with temperature and rainfall variations. *J. Geophys. Res. Atmos.* **115**: D14101, doi: 10.1029/2009JD012752.
- Piao SL, Fang JY, Zhou LM, Guo QH, Henderson M, Ji W, Li Y, Tao S. 2003. Interannual variations of monthly and seasonal normalized difference vegetation index (NDVI) in China from 1982 to 1999. *J. Geophys. Res.* **108**(D14): 4401, doi: 10.1029/2002JD002848.
- Piao SL, Fang JY, He JS. 2006a. Variations in vegetation net primary production in the Qinghai-Xizang Plateau, China, from 1982 to 1999. *Clim. Change* **74**(1–3): 253–267, doi: 10.1007/s10584-005-6339-8.
- Piao SL, Mohammat A, Fang JY, Cai Q, Feng JM. 2006b. NDVI-based increase in growth of temperate grasslands and its responses to climate changes in China. *Glob. Environ. Change* **16**(4): 340–348, doi: 10.1016/j.gloenvcha.2006.02.002.
- Piao SL, Wang XH, Ciais P, Zhu B, Wang T, Liu J. 2011. Changes in satellite-derived vegetation growth trend in temperate and boreal Eurasia from 1982 to 2006. *Glob. Change Biol.* **17**(10): 3228–3239, doi: 10.1111/j.1365-2486.2011.02419.x.
- Potter C, Boriah S, Steinbach M, Kumar V, Klooster S. 2008. Terrestrial vegetation dynamics and global climate controls. *Clim. Dyn.* **31**(1): 67–78, doi: 10.1007/s00382-007-0339-5.
- Rocchini D. 2007. Effects of spatial and spectral resolution in estimating ecosystem α -diversity by satellite imagery. *Remote Sens. Environ.* **111**(4): 423–434, doi: 10.1016/j.rse.2007.03.018.
- Ruse JW, Haas RH, Schell JA, Deering DW, Harlan JC. 1974. Monitoring the vernal advancements and retrogradation of natural vegetation. Final Report, NASA/GSFC, Greenbelt, MD, 1–137.
- Schmidt M, Klein D, Conrad C, Dech S, Paeth H. 2014. On the relationship between vegetation and climate in tropical and northern Africa. *Theor. Appl. Climatol.* **115**(1–2): 341–353, doi: 10.1007/s00704-013-0900-6.
- Serreze M, Walsh J, Chapin IF, Osterkamp T, Dyurgerov M, Romanovsky V, Oechel W, Morison J, Zhang T, Parry R. 2000. Observational evidence of recent change in the northern high-latitude environment. *Clim. Change* **46**(1–2): 159–207, doi: 10.1023/A:1005504031923.
- Shinoda M. 1995. Seasonal phase lag between rainfall and vegetation activity in tropical Africa as revealed by NOAA satellite data. *Int. J. Climatol.* **15**(6): 639–656, doi: 10.1002/joc.3370150605.
- Steven MD, Malthus TJ, Baret F, Xu H, Chopping MJ. 2003. Inter-calibration of vegetation indices from different sensor systems. *Remote Sens. Environ.* **88**(4): 412–422, doi: 10.1016/j.rse.2003.08.010.
- Thornthwaite CW. 1948. An approach toward a rational classification of climate. *Geogr. Rev.* **38**: 55–94.
- Tomé A, Miranda P. 2004. Piecewise linear fitting and trend changing points of climate parameters. *Geophys. Res. Lett.* **31**(2): L02207, doi: 10.1029/2003GL019100.
- Toms JD, Lesperance ML. 2003. Piecewise regression: a tool for identifying ecological thresholds. *Ecology* **84**(8): 2034–2041.
- Tucker CJ, Slayback DA, Pinzon JE, Los SO, Myneni RB, Taylor MG. 2001. Higher northern latitude normalized difference vegetation index and growing season trends from 1982 to 1999. *Int. J. Biometeorol.* **45**(4): 184–190, doi: 10.1007/s00484-001-0109-8.
- Upton C. 2010. Living off the land: nature and nomadism in Mongolia. *Geoforum* **41**: 865–874.
- Walther GR, Post E, Convey P, Menzel A, Parmesan C, Beebee TJ, Fromentin JM, Guldberg H, Bairlein F. 2002. Ecological responses to recent climate change. *Nature* **416**(6879): 389–395, doi: 10.1038/416389a.
- Wang XH, Piao SL, Ciais P, Li JS, Friedlingstein P, Koven C, Chen AP. 2011. Spring temperature change and its implication in the change of vegetation growth in North America from 1982 to 2006. *Proc. Natl. Acad. Sci. U.S.A.* **108**(4): 1240–1245, doi: 10.1073/pnas.1014425108.
- Watson RT, Albritton DL. 2001. *Climate Change 2001: Synthesis Report*. Cambridge University Press: Cambridge, UK.
- Whitlock C, Bartlein PJ. 1997. Vegetation and climate change in north-west America during the past 125 kyr. *Nature* **388**(6637): 57–61, doi: 10.1038/40380.
- Wu TT, Li YR. 2013. Spatial interpolation of temperature in the United States using residual kriging. *Appl. Geogr.* **44**: 112–120.
- Yao J, He XY, Li XY, Chen W, Tao DL. 2012. Monitoring responses of forest to climate variations by MODIS NDVI: a case study of Hun River upstream, northeastern China. *Eur. J. For. Res.* **131**(3): 705–716, doi: 10.1007/s10342-011-0543-z.
- Zemlich A, Manthey M, Zerbe S, Oyunchimeg D. 2010. Driving environmental factors and the role of grazing in grassland communities: a comparative study along an altitudinal gradient in Western Mongolia. *J. Arid Environ.* **74**(10): 1271–1280, doi: 10.1016/j.jaridenv.2010.05.014.
- Zhang XY, Hu YF, Zhuang DF, Qi YQ, Ma X. 2009. NDVI spatial pattern and its differentiation on the Mongolian Plateau. *J. Geogr. Sci.* **19**(4): 403–415.
- Zhang YL, Gao JG, Liu LS, Wang ZF, Ding MJ, Yang XC. 2013. NDVI-based vegetation changes and their responses to climate change from 1982 to 2011: a case study in the Koshi River Basin in the middle Himalayas. *Glob. Planet. Change* **108**(2013): 139–148, doi: 10.1016/j.gloplacha.2013.06.012.
- Zhou LM, Tucker CJ, Kaufmann RK, Slayback D, Shabanov NV, Myneni RB. 2001. Variations in northern vegetation activity inferred from satellite data of vegetation index during 1981 to 1999. *J. Geophys. Res. Atmos.* **106**(D17): 20069–20083, doi: 10.1029/2000JD000115.
- Zou XK, Zhai PM. 2004. Relationship between vegetation coverage and spring dust storms over northern China. *J. Geophys. Res. Atmos.* **109**: D03104, doi: 10.1029/2003JD003913.